Theory of image formation and diffraction

CCEM Summer School 2016
at McMaster University
Hamilton
May 29 - June 3, 2016

Pierre Stadelmann
JEMS-SAAS
CH-3906 Saas-Fee
Switzerland

May 25, 2016

HRTEM and HRSTEM imaging

The theory of diffraction and image formation has been fully developed as early as the 19^{th} century (Augustin Jean Fresnel (1788-1827), Joseph von Fraunhofer (1787-1826), Ernst Karl Abbe (1840-1905)[1]) and provides the mathematical tools necessary to understand diffraction and image formation in electron microscopy. Some recommended books are:

- J.M. Cowley, *Diffraction Physics*.
- P.B. Hirsch, A. Howie, R.B. Nicholson, W.D. Pashley & M.I. Whelan, *Electron Microscopy of Thin Crystals*.
- J.-P. Morniroli, *Large-Angle Convergent-Beam Electron Diffraction*.
- S.J. Pennycook & P.D. Nellist, *Scanning Transmission Electron Microscopy*.
- J.C.H. Spence, *High Resolution Electron Microscopy*.
- Z.L. Wang, *Elastic and Inelastic Electron Scattering in Electron Diffraction and Imaging*.

Recommended articles:

- J.M. Cowley & A.F. Moodie, Acta Cryst. **10**, (1957) 609-619.
- D. Gratias & R. Portier, Acta Cryst. **A39** (1983) 576-584.
- K. Ishizuka, Ultramicroscopy **5** (1980) 55-65, Ultramiscoscopy **90** (2002) 71-83.
- D. Van Dyck, Phys. Status Solidi **72** (1975) 321-336.

[1] J.W. Goodman, *Introduction to Fourier Optics*, McGraw-Hill Book Company (1968).

HR(S)TEM image simulation

The theory of image formation and diffraction is the foundation of HR(S)TEM diffraction and image simulation. These simulations are very often necessary to properly interpret and analyse the experimental images.

- **Simple structure: Co**
- **More complicated structure:** $MgZn_2$
- **Complicated structure:** $Cr_3Ni_5Si_2$

The first structure is very simple but hexagonal. In hexagonal crystals (hkl) plane normals are not parallel to [uvw] directions where (h=u, k=v & l=w) (except (001) // [001]).

Simple structure: Co

When simple structures are imaged, image simulation may not be necessary at all. For example looking at Co (P63/mmc, magnetic!), model structure, projected potential, SAED, HRTEM are simple (and straight forward to interpret?):

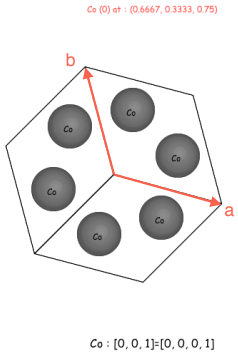

Model structure Cobalt, [001].

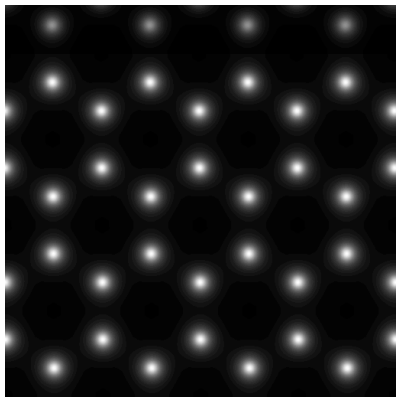

Projected potential Co [001]

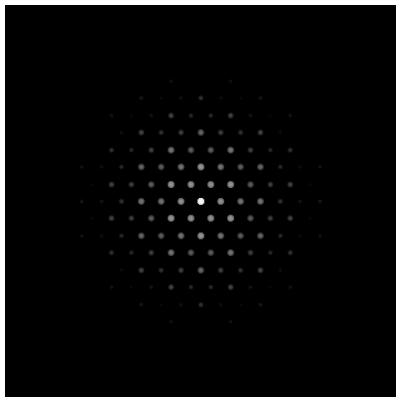

Selected Area Electron Diffraction (SAED) Co [001].

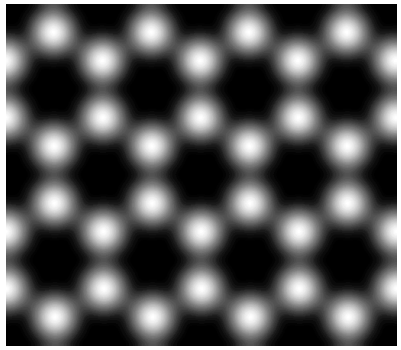

HRTEM image Co [001], Titan negative Cs.

More complicated structure: $MgZn_2$

When moderately complicated structures are imaged, image simulation may still not be necessary. For example looking at $MgZn_2$ (P63/mmc), model structure, projected potential, SAED, HRTEM are simple (SAED straight forward to interpret?):

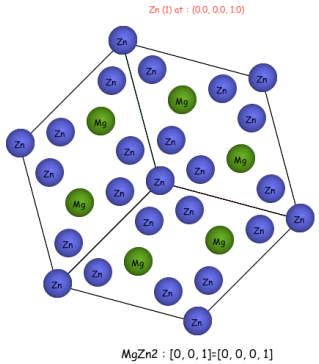

Model structure $MgZn_2$, [001].

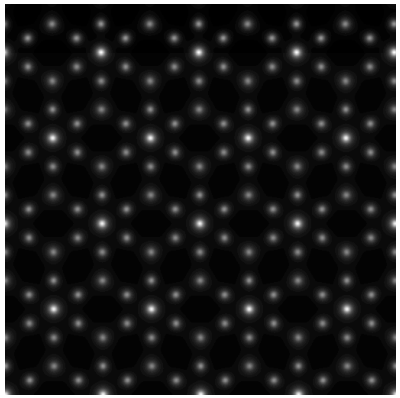

Projected potential $MgZn_2$ [001]

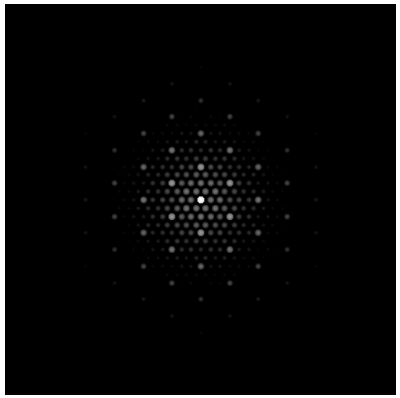

Selected Area Electron Diffraction (SAED) $MgZn_2$ [001].

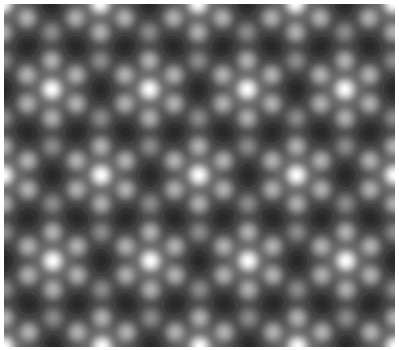

HRTEM image $MgZn_2$ [001], Titan negative Cs.

Co observed in [120] projection (Weber notation [10-10])

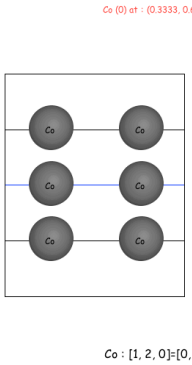

Model structure Cobalt, [120].

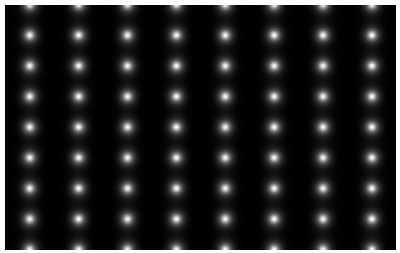

Projected potential Co [120]

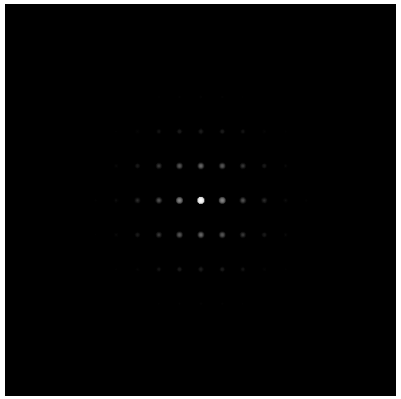

Selected Area Electron Diffraction (SAED) Co [120].

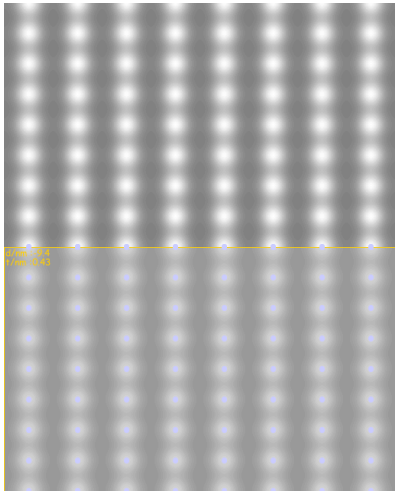

HRTEM image Co [120], Titan negative Cs.

$MgZn_2$ observed in [120] projection (Weber notation [10-10])

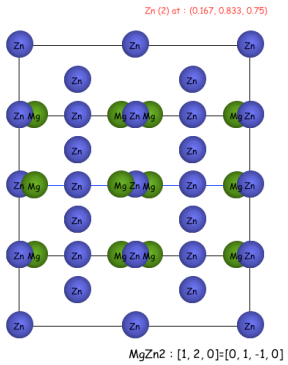

Model structure $MgZn_2$, [120].

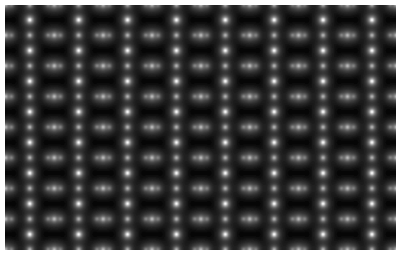

Projected potential $MgZn_2$ [120]

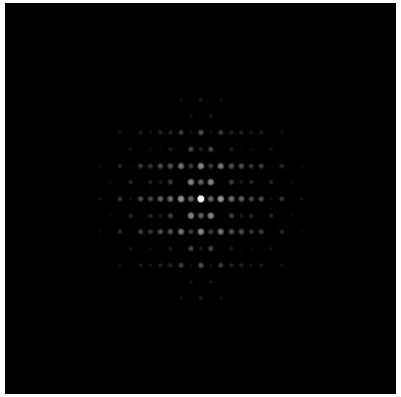

Selected Area Electron Diffraction (SAED) $MgZn_2$ [120].

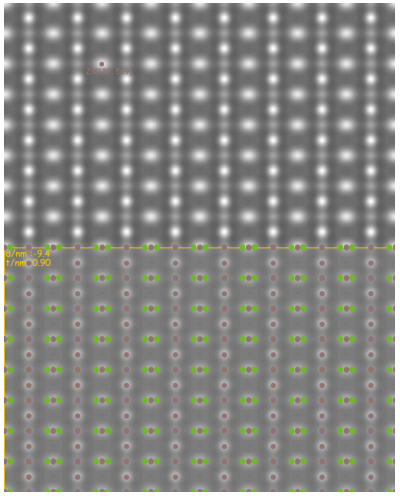

Figure: HRTEM image $MgZn_2$ [120], Titan negative Cs.

Complicated structure: $Cr_3Ni_5Si_2$ observed in [001] projection

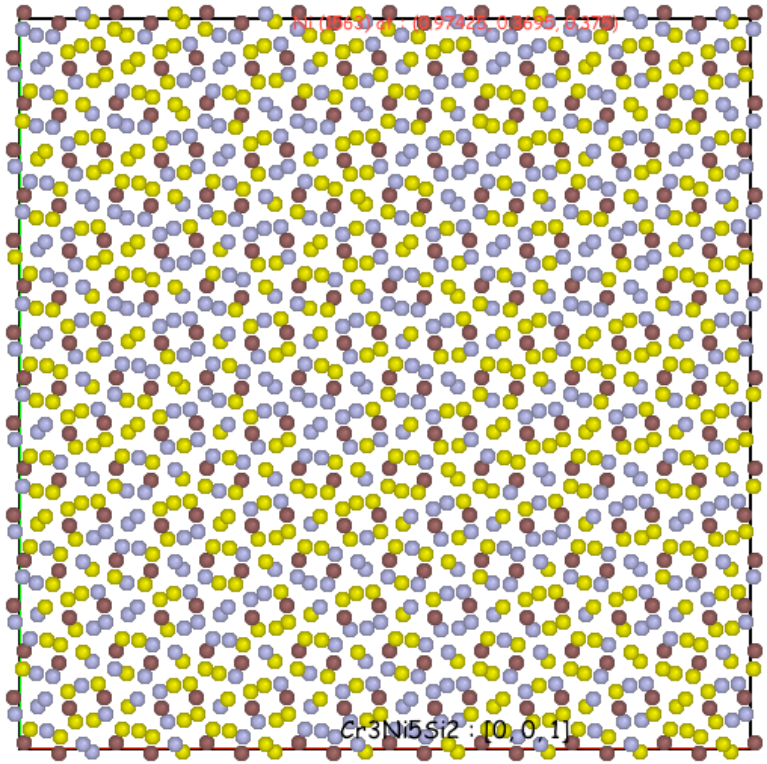

Model structure $Cr_3Ni_5Si_2$, [001].

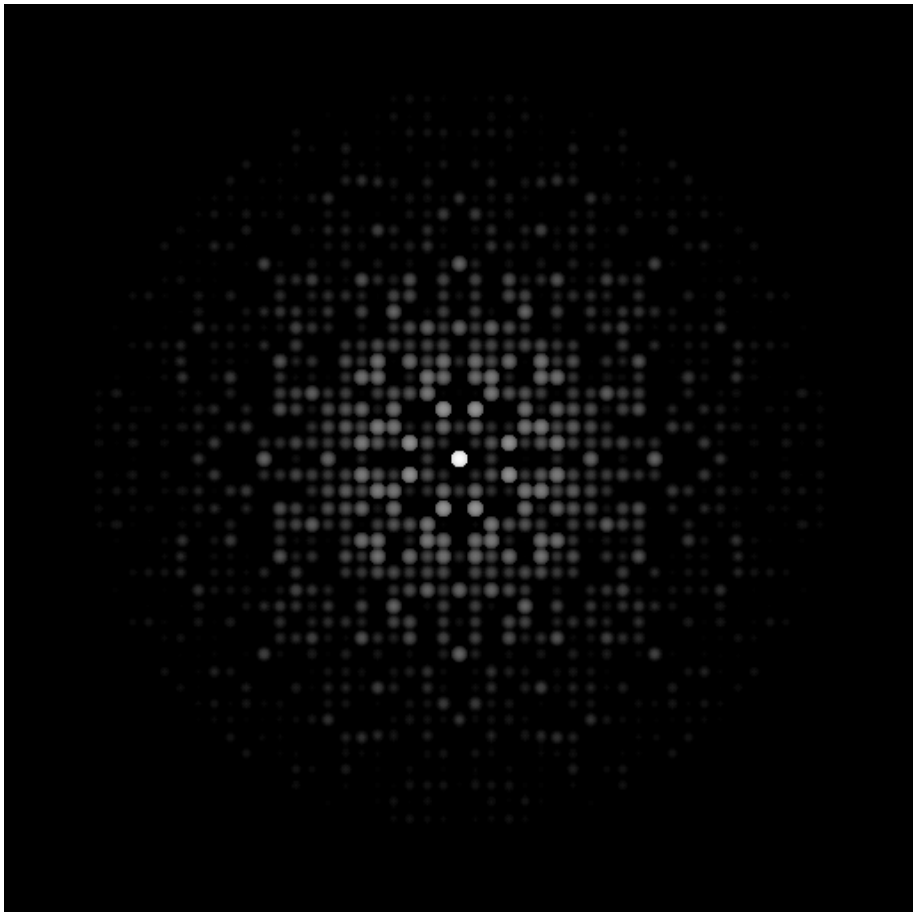

Selected Area Electron Diffraction (SAED) $Cr_3Ni_5Si_2$ [001]

$Cr_3Ni_5Si_2$ observed in [001] projection

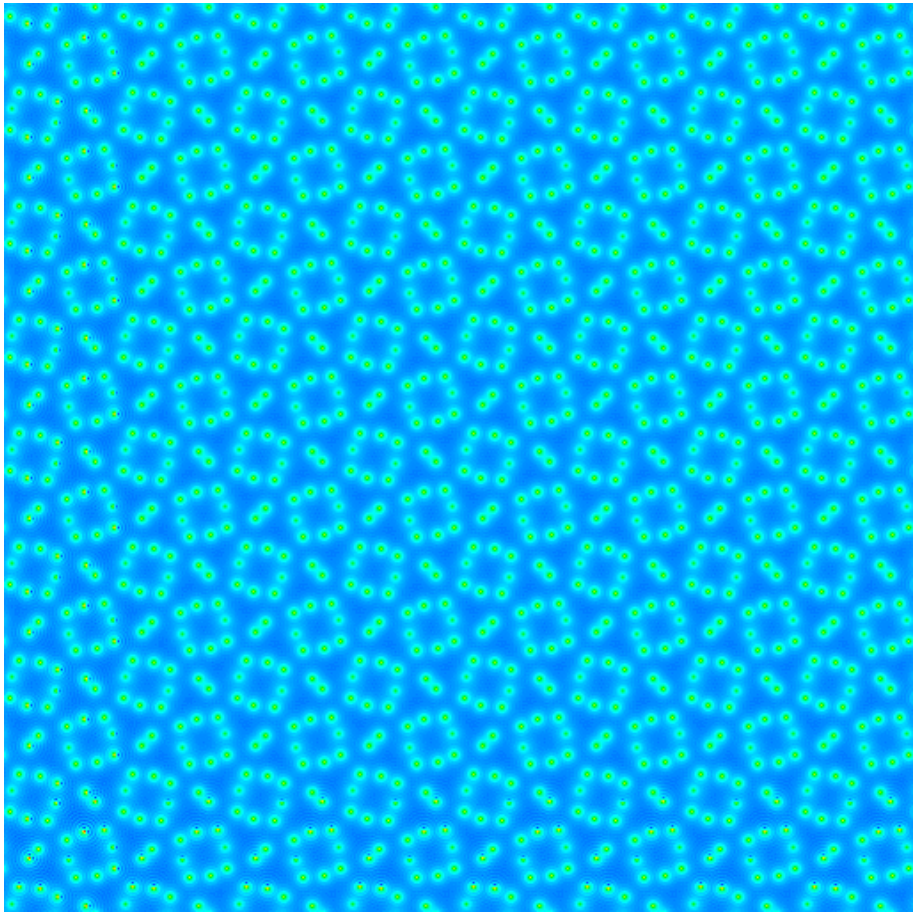

Projected potential $Cr_3Ni_5Si_2$ [001].

HRTEM image $Cr_3Ni_5Si_2$ [001], Titan negative Cs.

$Cr_3Ni_5Si_2$ observed in [001] projection

Imaging a thicker crystal or changing defocus modify (in general) the HRTEM images (where are the atomic columns?).

HRTEM image $Cr_3Ni_5Si_2$ [001], thickness 10 nm, defocus -8.2 nm.

HRTEM image $Cr_3Ni_5Si_2$ [001], thickness 10 nm, defocus 8.2 nm.

$Cr_3Ni_5Si_2$ observed in [001] projection

Imaging a thicker crystal or changing defocus modify (in general) the HRTEM images (where are the atomic columns?).

HRTEM image $Cr_3Ni_5Si_2$ [001], thickness 10 nm, defocus -8.2 nm.

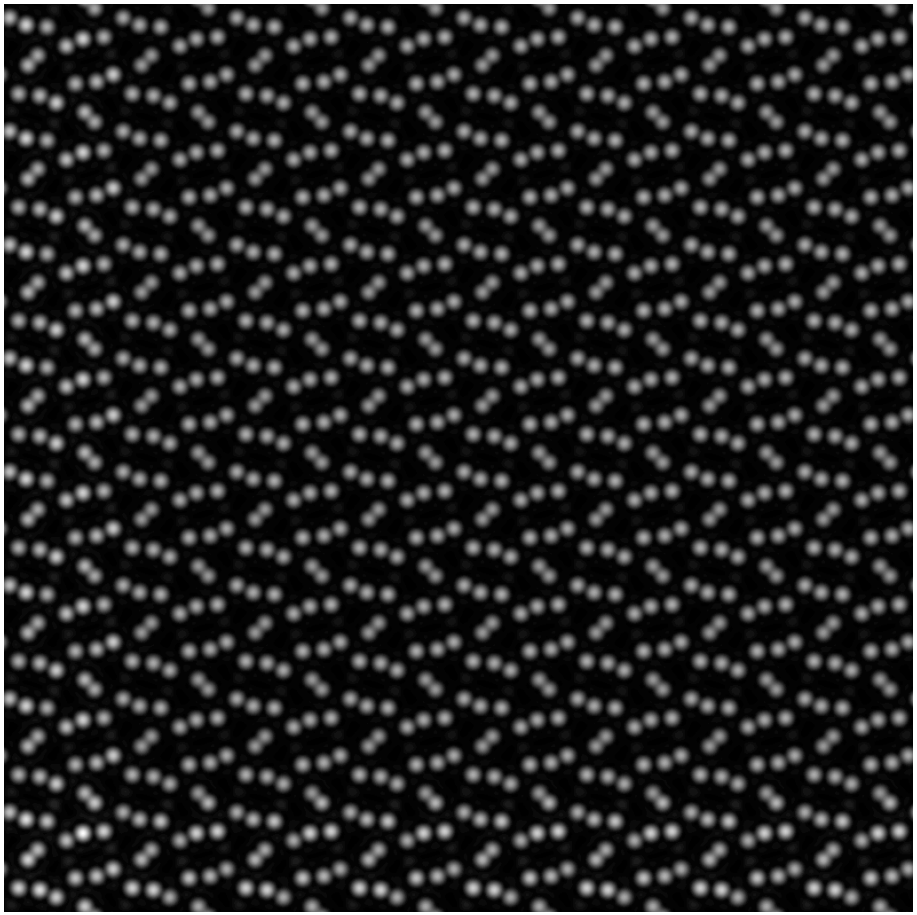

HAADF image $Cr_3Ni_5Si_2$ [001], thickness 10 nm.

$Cr_3Ni_5Si_2$ observed in [001] projection

Imaging a thicker crystal or changing defocus modify (in general) the HRTEM images (where are the atomic columns?).

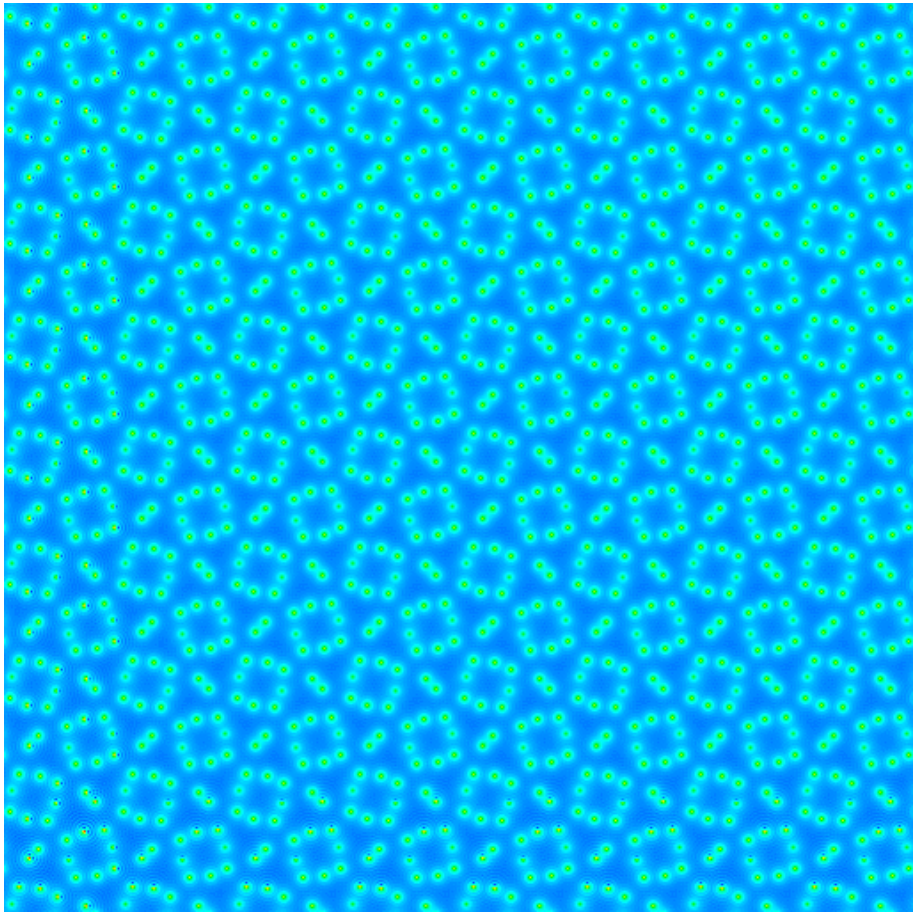

Projected potential $Cr_3Ni_5Si_2$ [001].

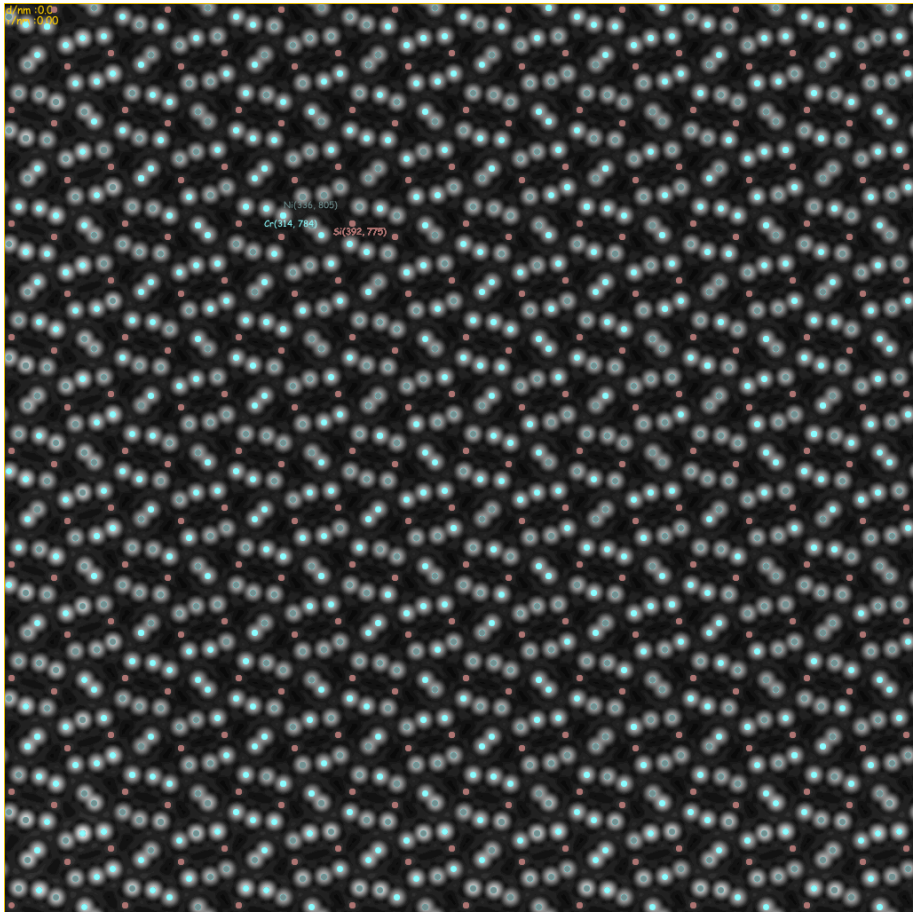

HAADF image $Cr_3Ni_5Si_2$ [001], thickness 10 nm.

Theory of image formation and diffraction in the electron microscope

We need models, (good) approximations.

1. **Models**
   - 1.1 **Crystal or ...**
     - Lattice parameters.
     - Symmetries (space-group, regular point system).
     - Atoms position.
     - Orientation, ([uvw] zone axis indices, (hkl) Laue circle center indices with u h + v k + w l = 0).
     - Shape (thickness, defect, ...).
   - 1.2 **Microscope**
     - Source coherence (i.e. size, energy spread).
     - Accelerating voltage.
     - Objective lens properties (Cs: spherical aberration coefficient, Cc: chromatic aberration coefficient, ...).
   - 1.3 **Detector**: Modulation Transfer Function (MTF).

2. **Approximations for diffraction**
   - 2.1 Elastic scattering (under small angle scattering approximation, i.e. acc. voltage $\geq$ 50 kV):
     - Kinematical: single scattering event.
     - Dynamical: multiple scattering events.
   - 2.2 Inelastic scattering:
     - Single inelastic scattering.
     - Multiple inelastic scattering.
     - Frozen lattice or frozen phonon.

3. **Approximations for image formation**
   - 3.1 Abbe imaging theory (transmission cross-coefficients or transfer function + envelopes).

Specimen crystalline, amorphous, both?

Books on crystallography that you may find useful:

- D.E. Sands, *Introduction to Crystallography*, Dover Books on Chemistry.
- D.E. Sands, *Vectors and Tensors in Crystallography*, Dover Publications Inc.

Models: specimen

Models are not necessarily crystalline.

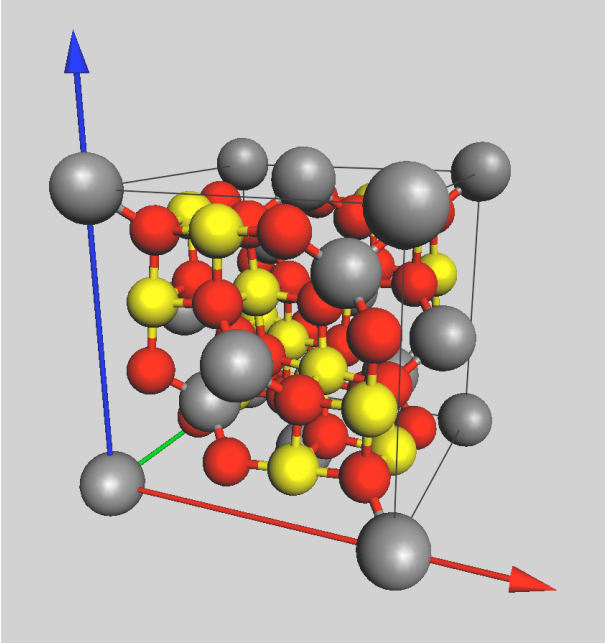

CoCr2O4 (cubic, F d -3 m, 3 atoms).

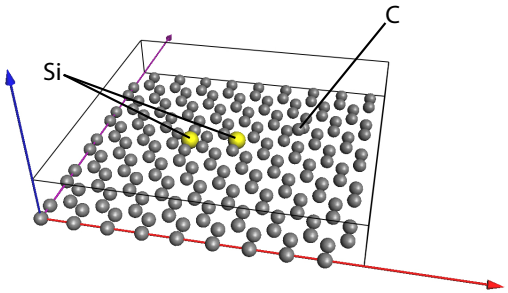

Graphene sheet with add atoms (448 atoms).

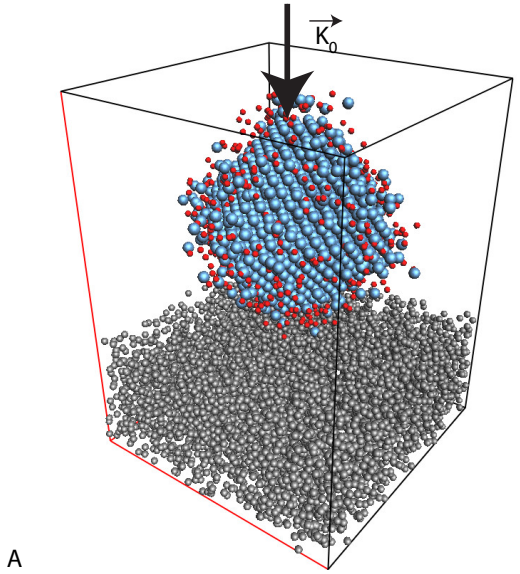

Pt catalyst (Pt cube octahedron on amorphous carbon film, 10'000 atoms).

A model is a box of parameters (a, b, c, α, β, γ) with atoms at (x,y,z) such that $0.0 \leq (x, y, z) < 1.0$. The symmetries (space-group) helps defining the structure, the extinctions, etc[2].

[2]Wrong models do not provide reliable HRTEM or HRSTEM simulated images.

Models: Paraxial optics and principal rays

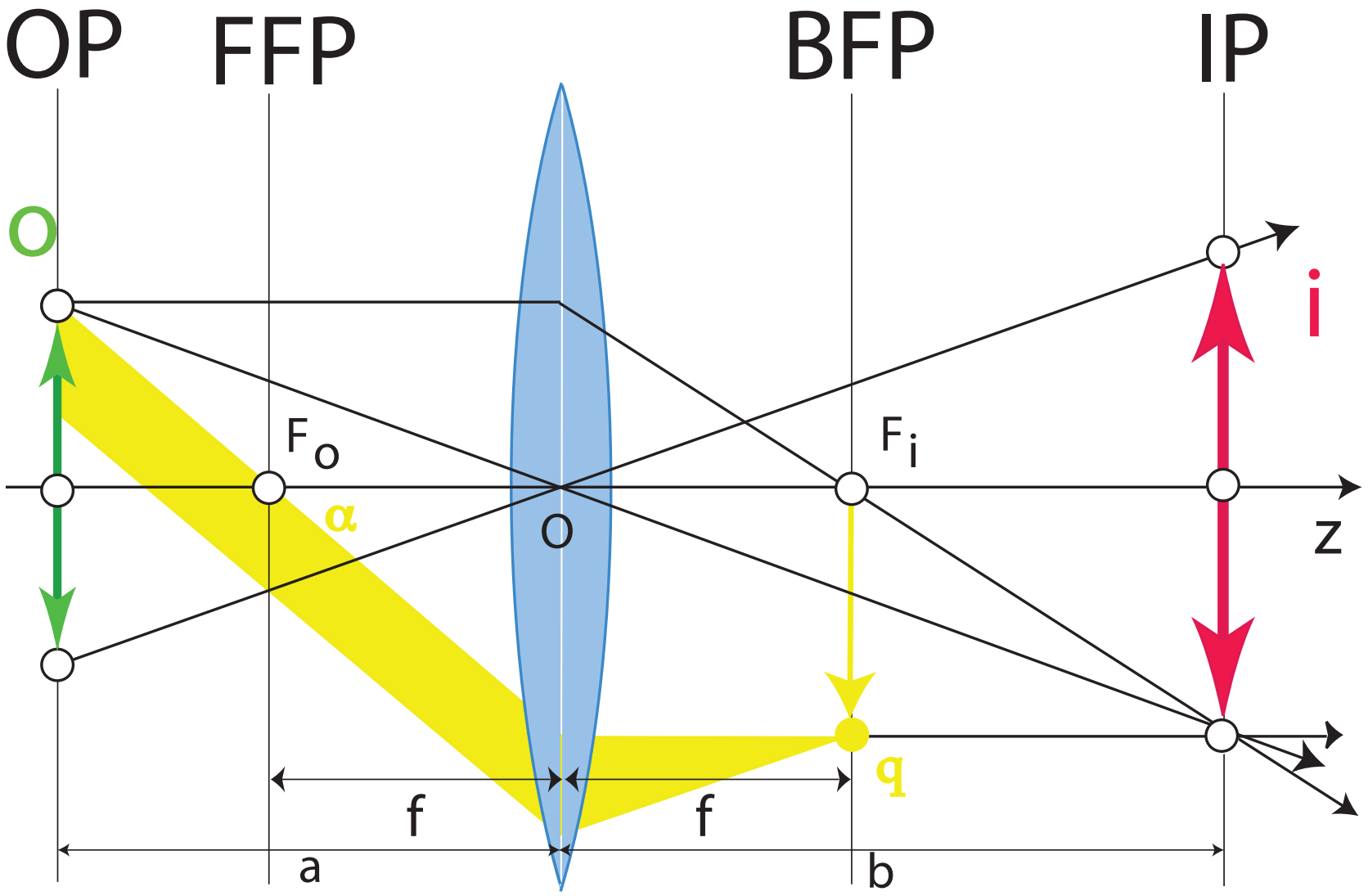

Principal rays of paraxial optics. Reflection (plane wave) making an angle α, where $\alpha = 2\theta_B$, corresponds to spatial frequency u.

Models: the electron microscope (paraxial optics or gaussian optics)

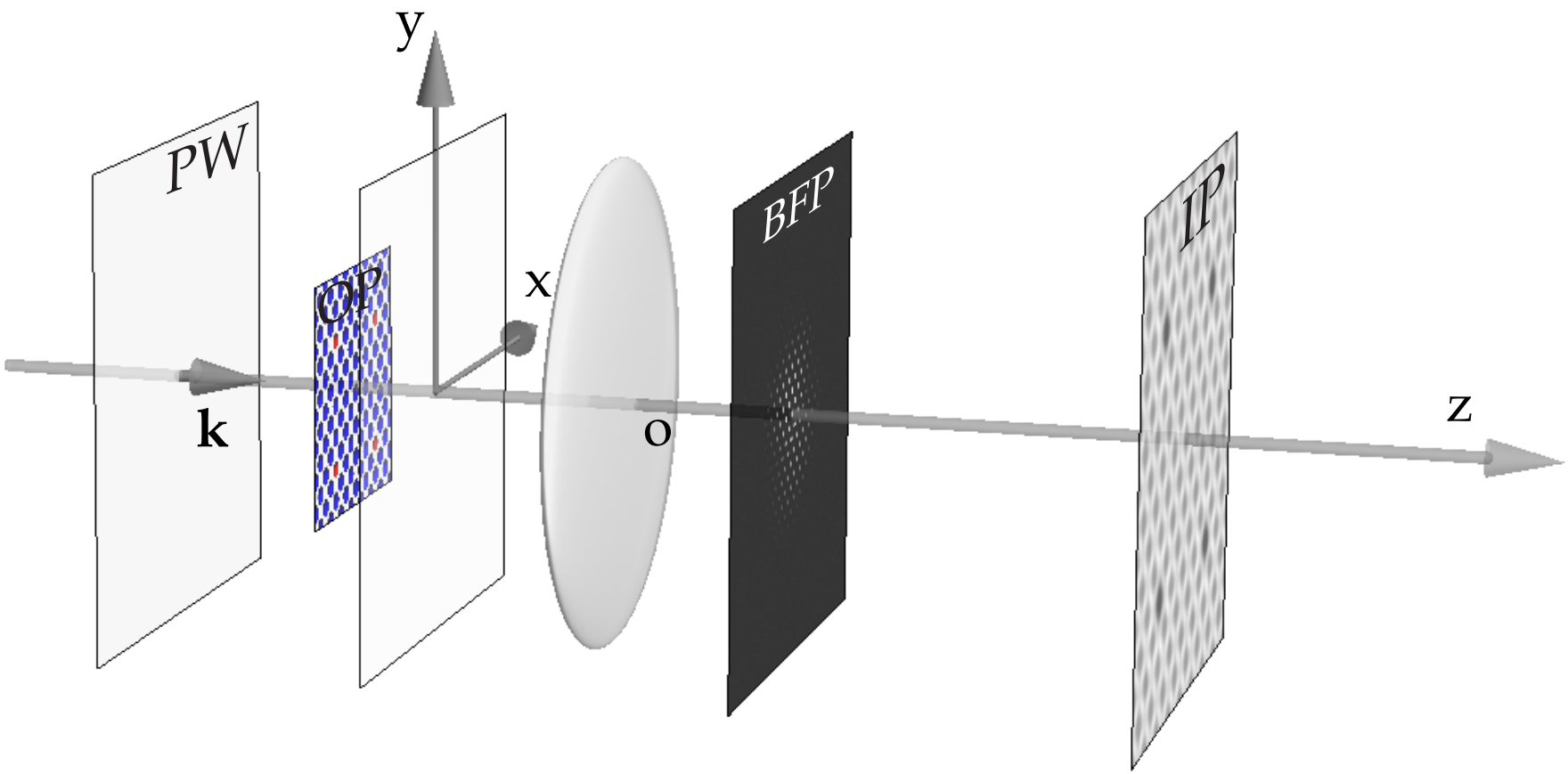

PW: incident Plane Wave, **OP**: Object Plane, **BFP**: Back Focal Plane, **IP**: Image Plane.
Only objective lens is modelled and axial aberrations considered[3][4].

[3]The objective lens is the first imaging lens and its lateral magnification G_l is very large (HRTEM).

[4]Angular compression G_a is the inverse of lateral magnification G_l ($G_l G_a = 1$).

Electron diffraction

- Small angle elastic scattering[5].
  - Kinematical diffraction (single scattering event).
  - Dynamical diffraction (multiple scattering events).
- Inelastic scattering.
  - Single scattering event.
  - Multiple scattering events.

Imaging

- Coherent illumination (mono kinetic electrons and point source).
- Incoherent illumination (scanning).
- Partially coherent illumination.
  - Coherent illumination + attenuation envelopes.
  - Transmission cross-coefficients.

[5]Small angle scattering has been shown to be a good approximation for electrons of energy larger than 50 KeV.

Approximations: elastic scattering

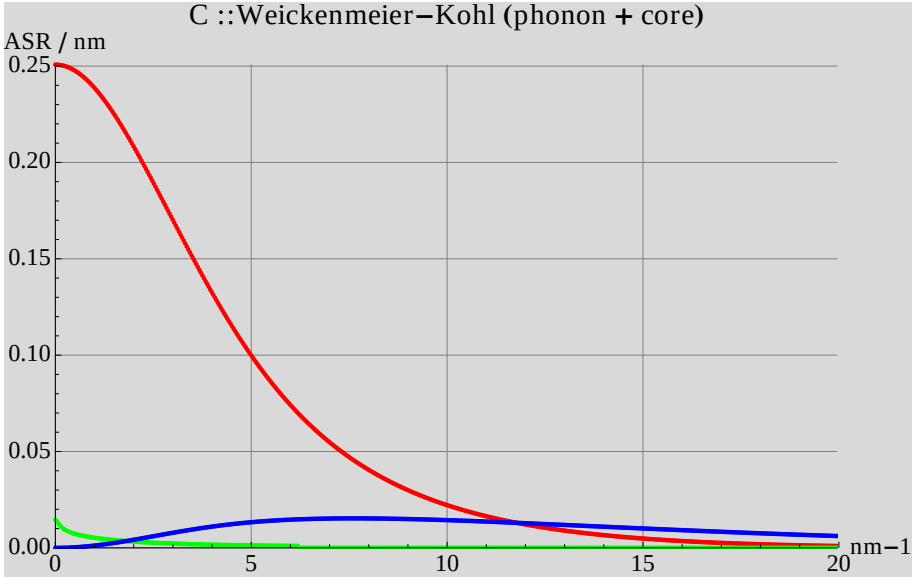

Atomic Scattering Amplitude (carbon), red: elastic, green: core absorption, blue: TDS (Thermal Diffuse Scattering).

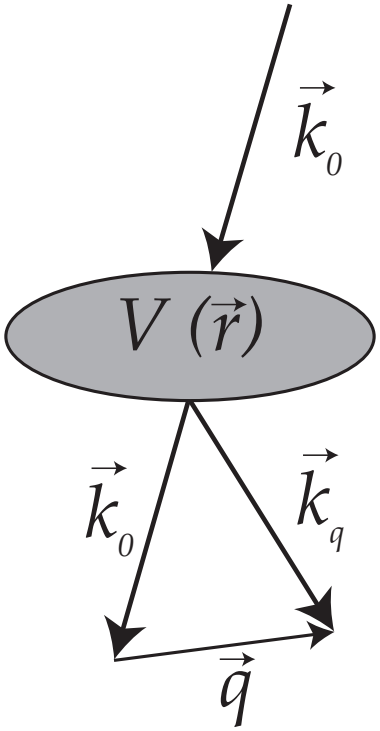

Electrons interact with the crystal potential $V(\vec{r})$.

Scattering:

$$\vec{k}_q = \vec{k}_o + \vec{q}$$

Elastic scattering:

$$||\vec{k}_q|| = ||\vec{k}_o||$$

Approximations: Abbe image formation

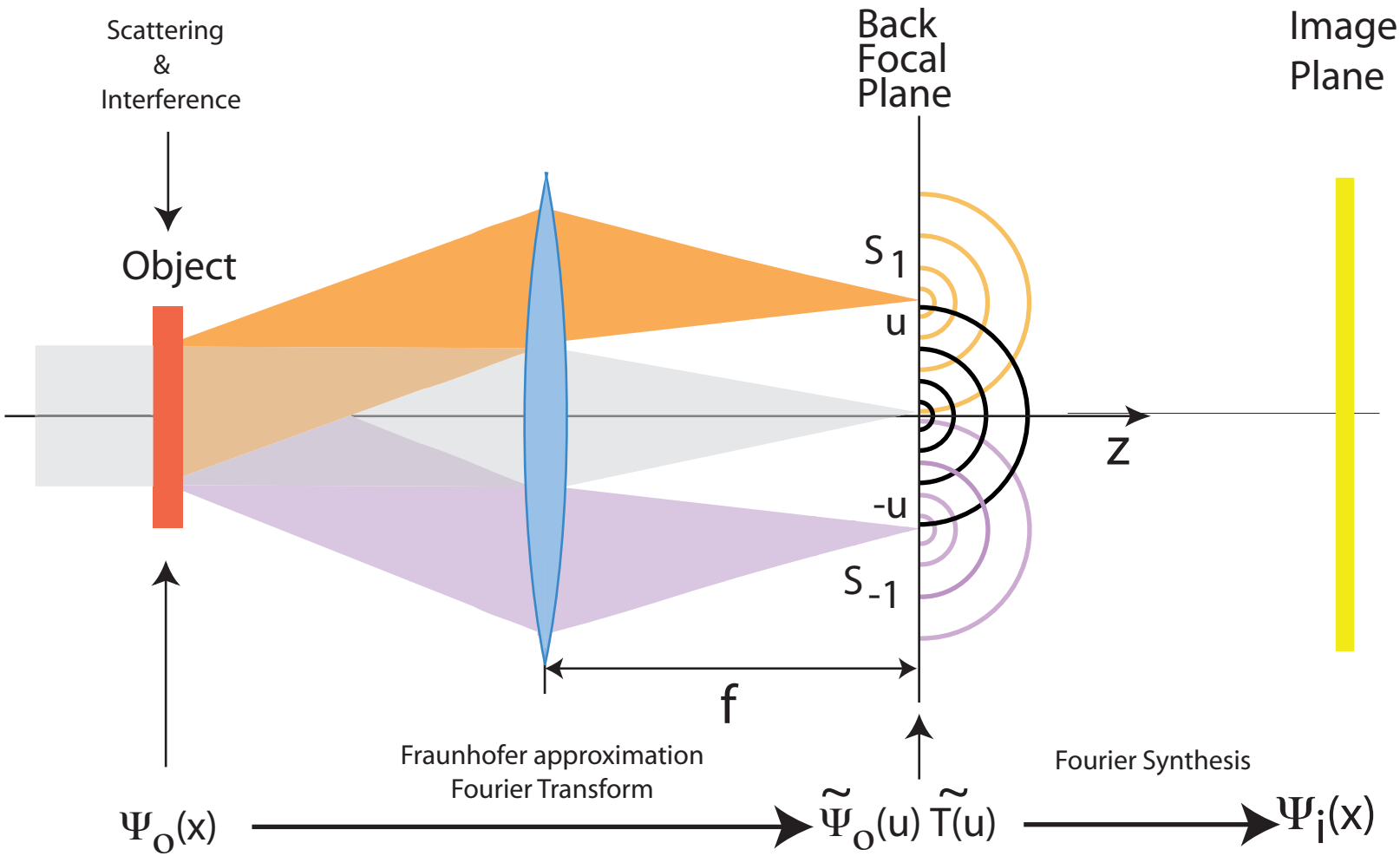

The objective lens changes the phase relationship between the transmitted and diffracted beams. Moreover not all diffracted beams are transmitted, due to its small acceptance angle. High spatial frequencies (i.e. beams diffracted at large angles are damped due to partial spatial and temporal coherence, electronic noise, mechanical vibrations or drift.

Approximations: transfer function $\tilde{T}(\vec{u})$

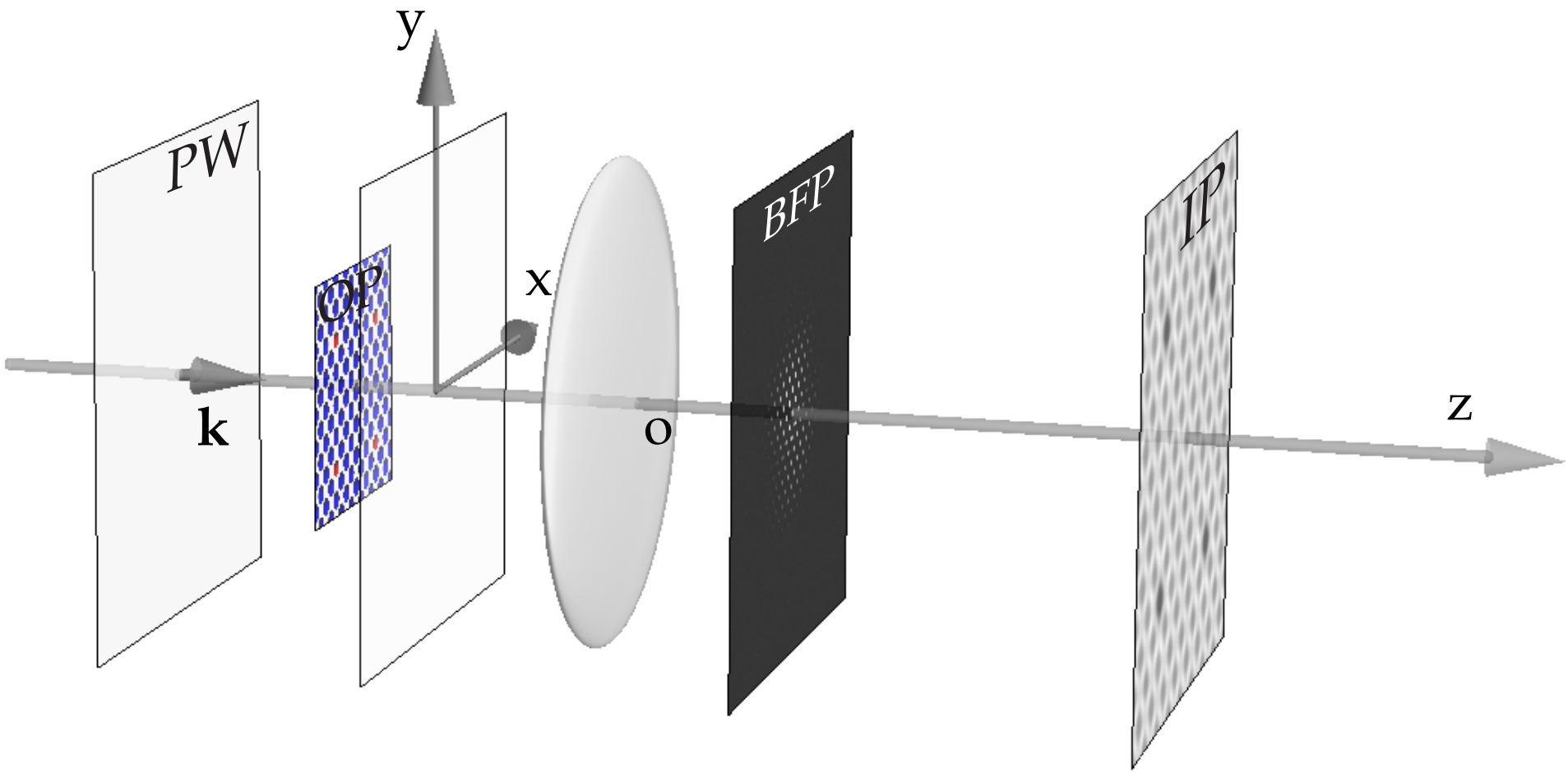

The electron microscope transfer is modelled by a transfer function $\tilde{T}(\vec{u})$ that acts only in its Back Focal Plane (BFP). The BFP is the plane where the Fourier transform of the object wave function $\tilde{\Psi}_o(\vec{u})$ is formed. In the Image Plane, the image intensity is $\Psi_i(\vec{x})\ \Psi_i(\vec{x})^*$ i.e. the modulus square of the image wave function $\Psi_i(\vec{x})$.

Mathematics of the theory of image formation and diffraction

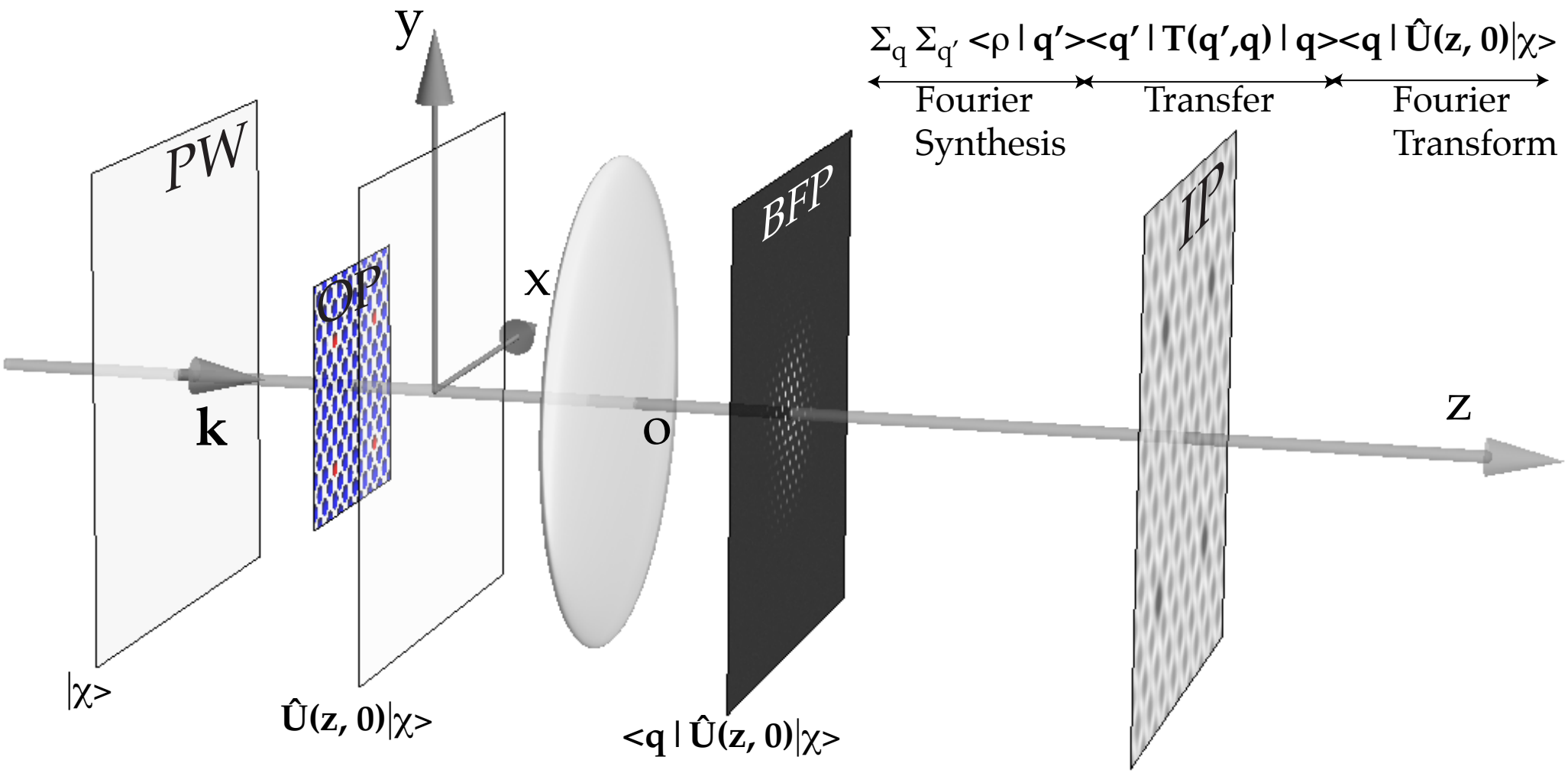

Image wave function: $|\Psi_i>$

$$|\chi> \implies \text{incident wave function}$$

$$|\Psi_i> = \underbrace{\sum^{q'} <\rho|q'>}_{\text{Fourier synthesis}} \underbrace{\sum^{q} <q'|T(q',q)|q>}_{\text{Objective lens transfer}} \underbrace{<q|U(z,0)|\chi>}_{\text{Fourier transform}}$$

Assuming that the potential is z independent, the evolution operator $U(z,0)$ depends on the Hamiltonian $H(\vec{\rho},z)$ of the system "crystal + incident electron" (where $\vec{\rho}$ are the (x, y) coordinates in a plane perpendicular to the optical axis O_z of the microscope):

$$U(z,0) = \exp^{-i\int_0^z H(\vec{\rho},z)dz}$$

The main problem of high-energy electron diffraction and imaging is to determine $U(z,0)$[6].

[6] First solution by Hans Albrecht Bethe, *Theory of the Diffraction of Electrons by Crystals*, Ann. Phys. **87** (1928) 55-129.

Gratias & Portier: small angle & elastic scattering approximations

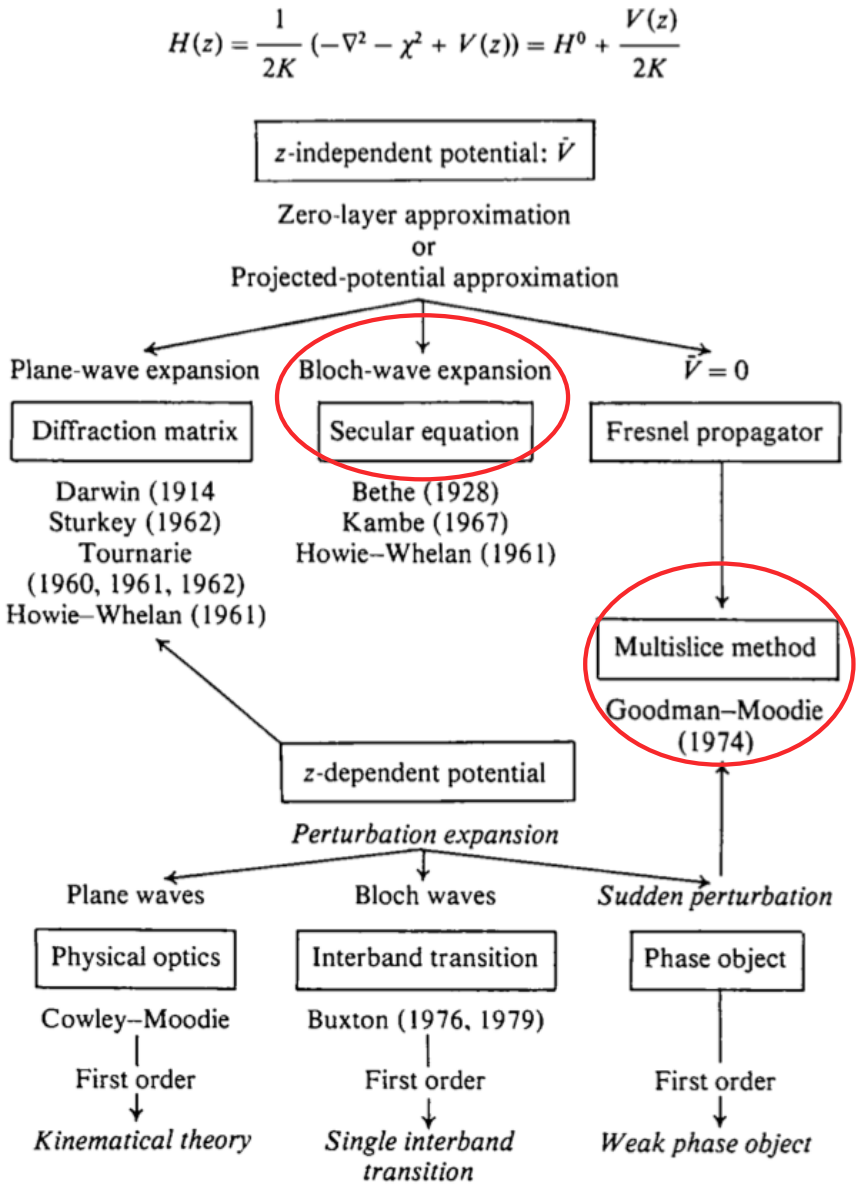

From Gratias and Portier[7].

[7] D. Gratias and R. Portier, Time-Like Perturbation Method in High-Energy Electron Diffraction, Acta Cryst. **A39** (1983) 576-584

Transfer by the objective lens: $< q' | \widetilde{T}(q', q) | q >$

Image forming system **S** has 2 properties (Abbe theory)[8]:

- Linear.
- Space invariant.

[8] $\Psi_i(\vec{x}) = S\{\Psi_o(\vec{x})\}$.

Linearity

$$
\begin{aligned}
S\{a_1\Psi_o^1(\vec{x}) + a_2\Psi_o^2(\vec{x})\} &= a_1 S\{\Psi_o^1(\vec{x})\} + a_2 S\{\Psi_o^2(\vec{x})\} \\
S\{a_1\Psi_o^1(\vec{x}) + a_2\Psi_o^2(\vec{x})\} &= a_1\Psi_i^1(\vec{x}) + a_2\Psi_i^2(\vec{x})
\end{aligned}
$$

$$
\Psi_o(\vec{x}) = \int_{-\infty}^{\infty} \Psi_o(\vec{u})\delta(\vec{x} - \vec{u})\mathrm{d}\vec{u}
$$

$$
\Psi_i(\vec{x}) = S\left\{\int_{-\infty}^{\infty} \Psi_o(\vec{u})\delta(\vec{x} - \vec{u})\mathrm{d}\vec{u}\right\}
$$

$$
\Psi_i(\vec{x}) = \int_{-\infty}^{\infty} \Psi_o(\vec{u}) S\{\delta(\vec{x} - \vec{u})\}\mathrm{d}\vec{u}
$$

Impulse response of the optical system $T(\vec{x};\vec{u})$:

$$
T(\vec{x};\vec{u}) = S\{\delta(\vec{x} - \vec{u})\}
$$

The effects of the optical system's elements (lenses, apertures, ...) is known when the images of the point sources of P_o are specified.

Space invariance: invariance by translation

Space invariance is realised when the image of a point source **does not** depend on its position in the object plane. When the point source is translated in the object plane, its image moves similarly in the image plane.

$$T(\vec{x};\vec{u}) = T(\vec{x}-\vec{u})$$

The image function (complex) $\Psi_i(\vec{x})$ is consequently given by a convolution integral of the object function $\Psi_o(\vec{u})$ and the point spread function $T(\vec{x})$ of the optical system:

$$\Psi_i(\vec{x}) = \int_{-\infty}^{\infty} \Psi_o(\vec{u})\, T(\vec{x}-\vec{u})\mathrm{d}\vec{u} = \Psi_o(\vec{x}) \otimes T(\vec{x})$$

Its Fourier transform is:

$$\widetilde{\Psi}_i(\vec{h}) = \widetilde{\Psi}_o(\vec{h})\, \widetilde{T}(\vec{h})$$

Abbe image formation theory defines $\widetilde{T}(\vec{h})$ by means of **Optical Path Differences (OPD)**.

Remark: Transfer Function $\widetilde{T}(\vec{u})$ and Optical Transfer Function $\widetilde{OTF}(\vec{u})$

$\rightarrow$ **TEM** ($\widetilde{T}(\vec{u})$: Transfer Function):

$$\begin{aligned}\widetilde{\Psi}_i(\vec{u}) &= \widetilde{\Psi}_o(\vec{u})\,\widetilde{T}(\vec{u}) \\ \Psi_i(\vec{x}) &= \int \widetilde{\Psi}_o(\vec{u})\,\widetilde{T}(\vec{u}) e^{2\pi\imath\vec{u}\cdot\vec{x}} \mathrm{d}\vec{u}\end{aligned}$$

$\rightarrow$ **STEM** ($\widetilde{OTF}(\vec{u}) = \widetilde{T}(\vec{u}) \otimes \widetilde{T}(-\vec{u})$: Optical Transfer Function):

$$\begin{aligned}
I(\vec{x}) &= \left\langle \Psi_i(\vec{x};t)\Psi_i^*(\vec{x};t)\right\rangle \\
\Psi_i(\vec{x};t) &= \Psi_o(\vec{x};t) \otimes T(\vec{x}) \\
I(\vec{x}) &= \left\langle [\Psi_o(\vec{x};t) \otimes T(\vec{x})][\Psi_o^*(\vec{x};t) \otimes T^*(\vec{x})]\right\rangle && (\otimes \text{ convolution.}) \\
I(\vec{x}) &= [T(\vec{x})\,T^*(\vec{x})] \otimes \left\langle \Psi_o(\vec{x};t)\Psi_o^*(\vec{x};t)\right\rangle && (T(\vec{x}) \text{ is time independent.}) \\
\left\langle \Psi_o(\vec{x};t)\Psi_o^*(\vec{x};t)\right\rangle &= |\Psi_o(\vec{x})|^2 && (\text{complete spatial incoherence}) \\
I(\vec{x}) &= |\Psi_o(\vec{x})|^2 \otimes [T(\vec{x})\,T^*(\vec{x})] \\
I(\vec{x}) &= I_o(\vec{x}) \otimes OTF(\vec{x})
\end{aligned}$$

Perfect optical system

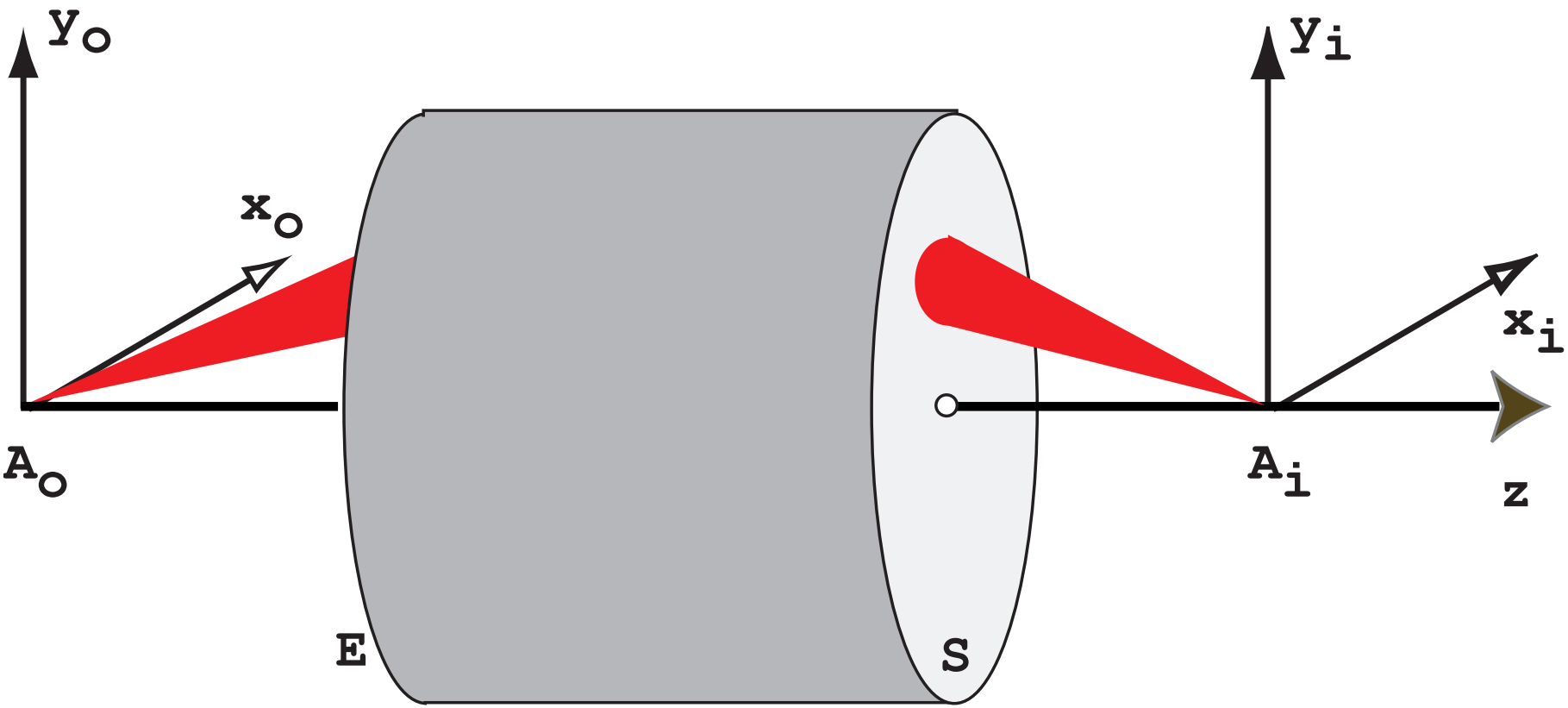

An optical system produces the image A_i of a point source object A_o. A_o and A_i are said to be conjugate. A_i is not a point since any optical system is diffraction limited. This limitation is introduced by the entrance and exit pupils of the optical system.

Aberrations of optical systems: how to define them

Some light rays emitted by object point A_o do not reach the image at point A_i.

Position of $A_i \longrightarrow$ intersection of the reference light ray (non deviated) and the image plane.

The image of a point source is a **spot** whose shape and intensity depend of the quality of the optical system.

Two types of aberrations:

1. Monochromatic.
2. Chromatic (λ dependent).

Pupils

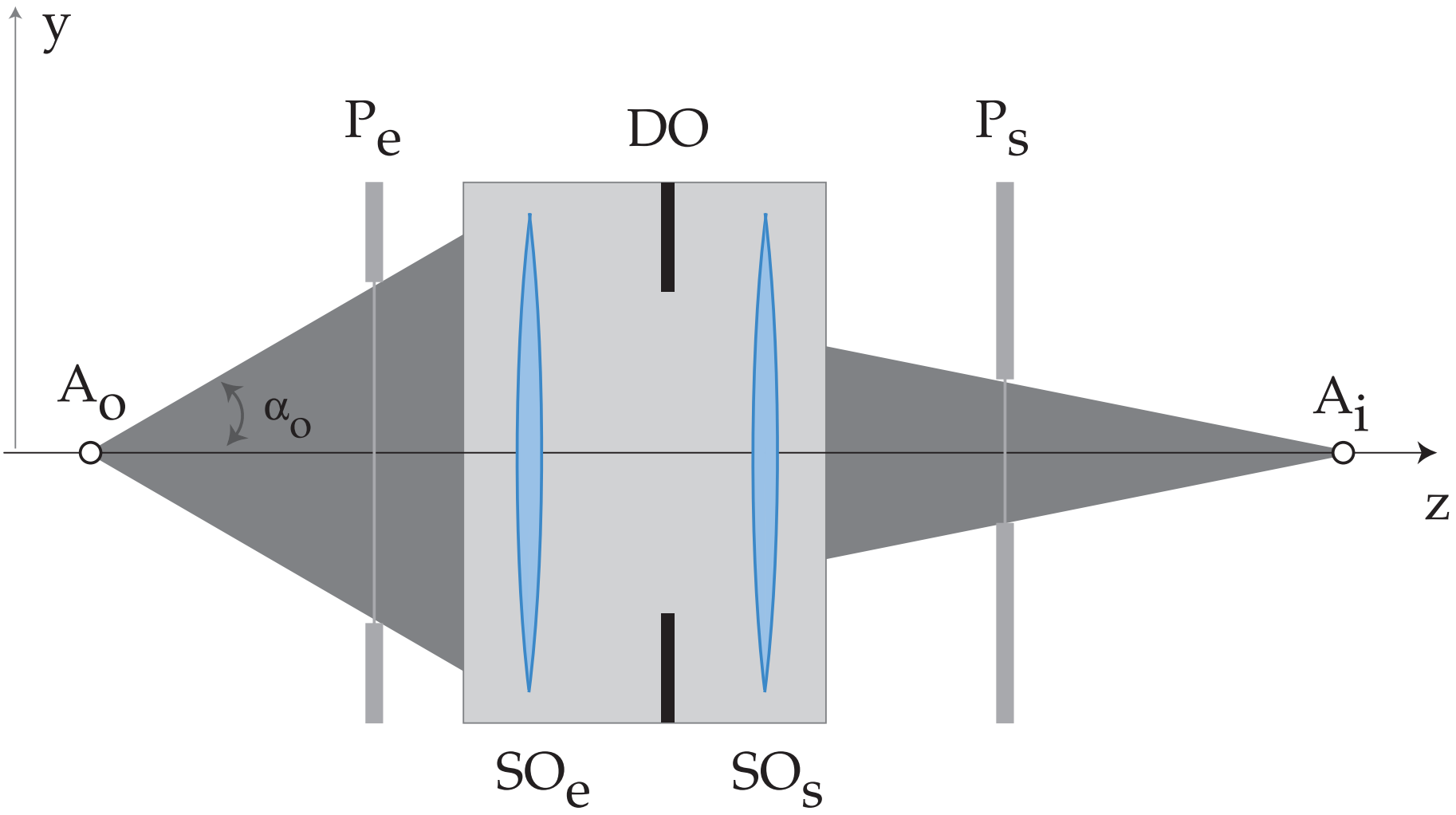

Any optical system can be characterised by an entrance pupil P_e and an exit pupil P_s. The pupils are the image of the opening aperture DO by the entrance and exit optical subsystems SO_e and SO_s. What are P_e and P_s for a thin lens?

Monochromatic aberrations

In order to evaluate the monochromatic aberrations one must define a function characteristic of the optical system.

This function will depend on:

1. The selected reference planes.
2. The optical path followed by the light ray.

Optical Path Length: OPL

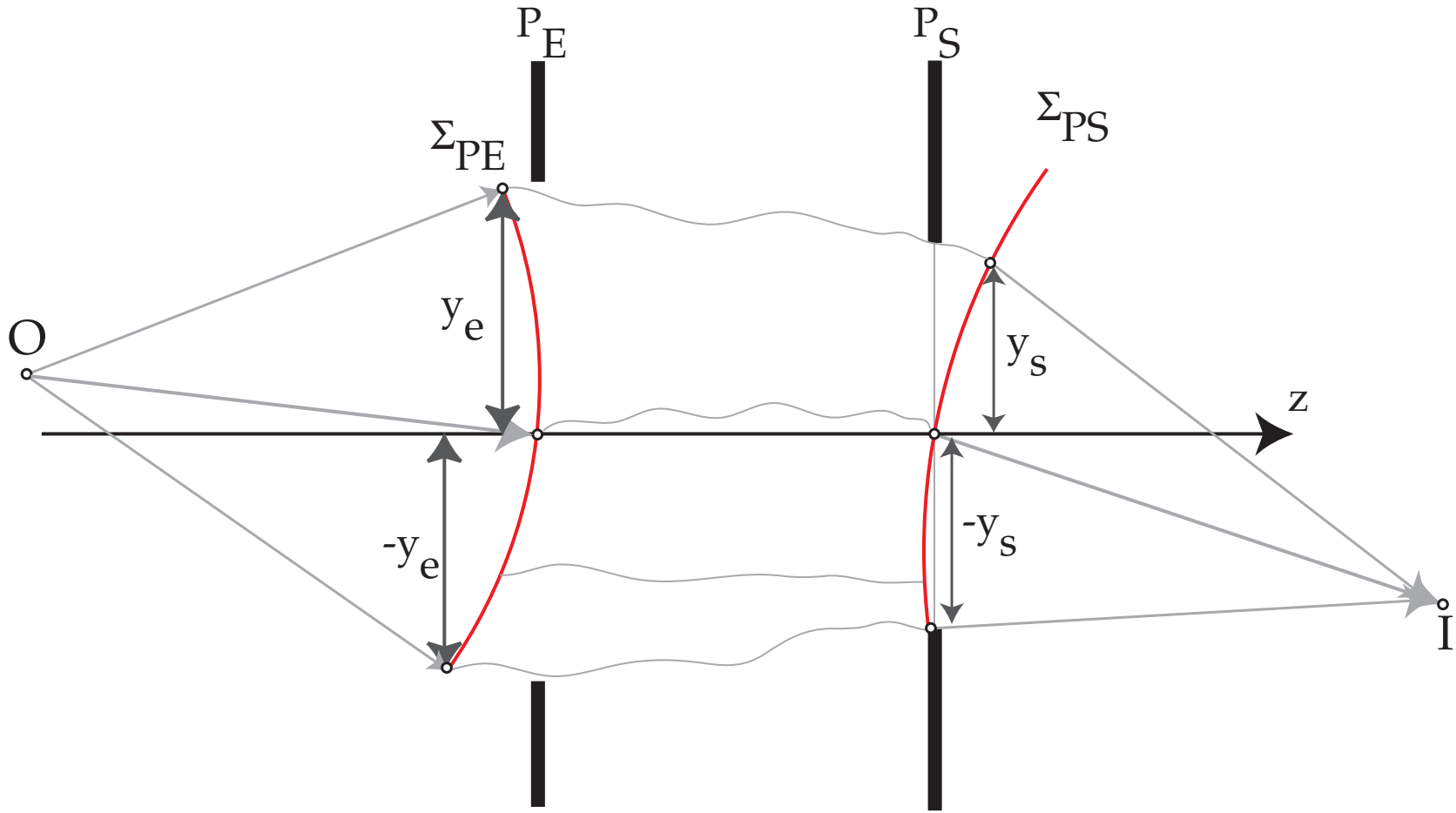

- Before P_E the reference wavefront Σ_{PE} is spherical (point source at O).
- After P_S the reference wavefront Σ_{PS} is spherical (converges towards I).

For a perfect optical system, both the entrance Σ_{PE} and exit Σ_{PS} wavefronts are spherical. The Optical Path Length form O to I is independent of the path.

Optical Path Difference (OPD): aberrations

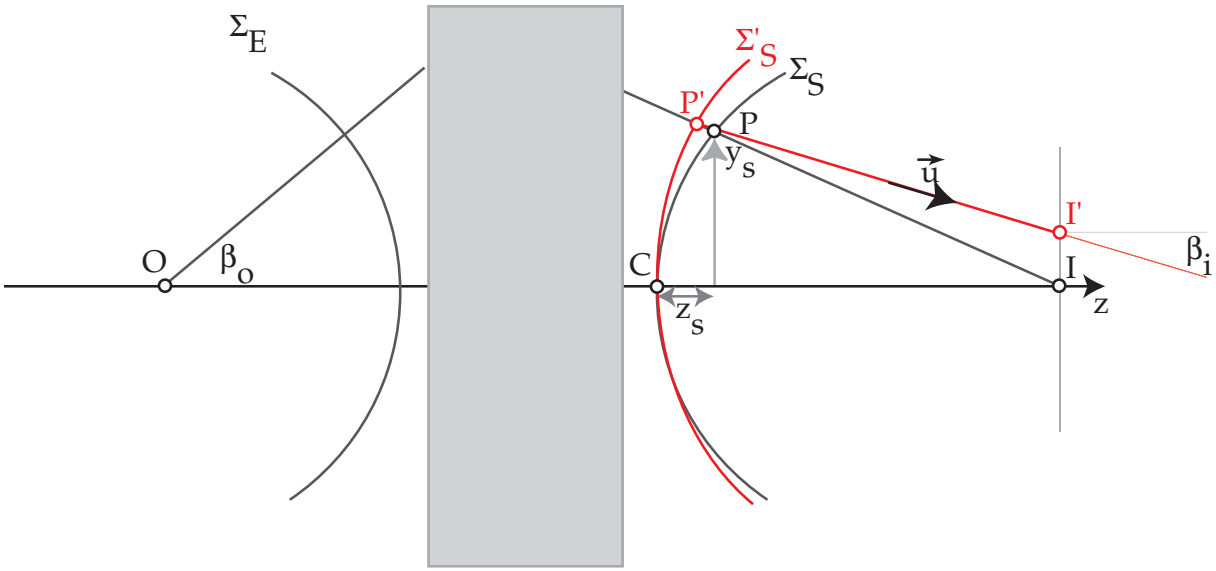

In the presence of aberrations the wavefront Σ'_S is no more spherical. The Optical Path Difference (distance between the deformed Σ'_S and spherical wavefront Σ_S) introduces a phase shift $\delta\phi$. With P' close to $P = (x_s, y_s)$ on reference sphere Σ_s, the OPD at $P' =$ (i.e. OPL from P' to P) is given by (Fermat principle):

$$W(x_s, y_s) = n_i \overline{P'P}$$

n_i refractive index of the medium $\longrightarrow$ phase shift:

$$\delta\phi = e^{2\pi\imath \frac{W(x_s, y_s)}{\lambda}}$$

Transverse geometric aberrations: $\vec{\epsilon}$

The transverse geometric aberrations are proportional to $\frac{d}{d\theta}$ wavefront aberrations[9]:

$$\epsilon_x = -\frac{f}{n_i}\frac{\partial W}{\partial x_s}$$
$$\epsilon_y = -\frac{f}{n_i}\frac{\partial W}{\partial y_s}$$

f focal length.

The OPD's introduced by all the aberrations of the imaging system are collected in a function $\chi(\vec{u})$ and the phase shift is[10]:

$$\widetilde{T}(\vec{u}) = e^{\imath\chi(\vec{u})}$$

$\widetilde{T}(\vec{u})$ has been first employed by Abbe in his description of image formation (1866).

[9] $P(x_s, y_s)$ on the spherical reference wavefront can be characterised by the radial angle θ.

[10] The angle θ corresponds (through Bragg law) to a spatial frequency $\vec{u}$, i.e. a distance in the back focal plane.

Optical Path Length: underfocus

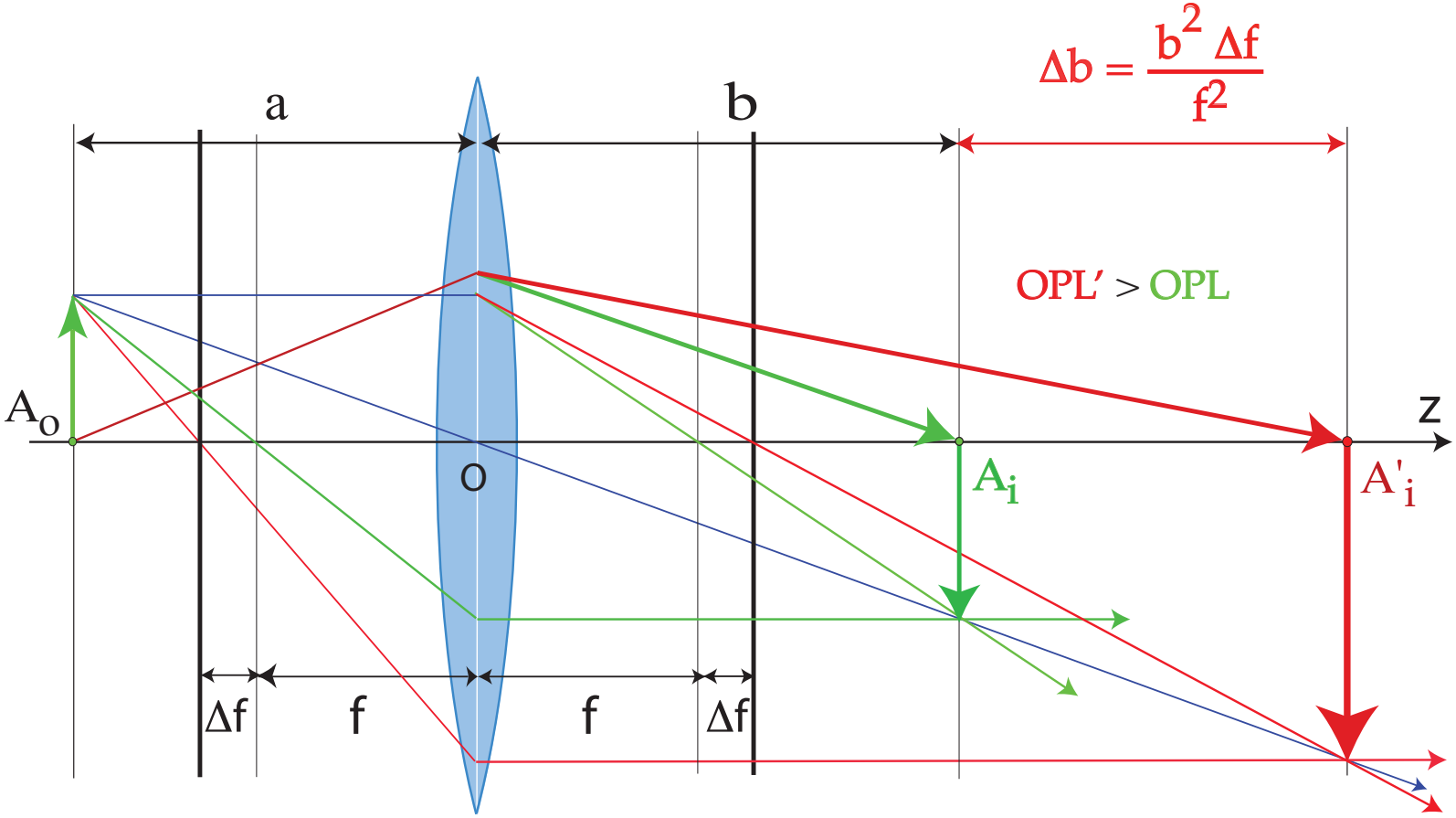

Underfocus weakens the objective lens, i.e. increases f. As a consequence the OPL from A_o to A'_i is larger:

$$e^{2\pi i \frac{\Delta f \lambda (\vec{q} \cdot \vec{q})}{2}}$$

Transfer function $T(\vec{q})$

$$T(\vec{q}) = e^{i\chi(\vec{q})} = \cos(\chi(\vec{q})) + i \underbrace{\sin(\chi(\vec{q}))}_{\text{Contrast transfer function}}$$

$$\chi(\vec{q}) = \pi \left[W_{20}\, \lambda\, \vec{q}.\vec{q} + W_{40} \frac{\lambda^3 (\vec{q}.\vec{q})^2}{2} + ... \right]$$

Where:

- W_{20} : defocus (z)
- W_{40}: spherical aberration (C_s)

Wave-front aberrations to 6^{th} order (cartesian coordinates)

$\{z, \pi\left(u^2+v^2\right)\lambda\}$ (*defocus*)
$\{W(1,1), 2\pi(u\cos(\phi(1,1))+v\sin(\phi(1,1)))\}$
$\{W(2,2), \pi\lambda((u-v)(u+v)\cos(2\phi(2,2))+2uv\sin(2\phi(2,2)))\}$
$\left\{W(3,1), \frac{2}{3}\pi\left(u^2+v^2\right)\lambda^2(u\cos(\phi(3,1))+v\sin(\phi(3,1)))\right\}$
$\left\{W(3,3), \frac{2}{3}\pi\lambda^2\left(u\left(u^2-3v^2\right)\cos(3\phi(3,3))-v\left(v^2-3u^2\right)\sin(3\phi(3,3))\right)\right\}$
$\left\{W(4,0), \frac{1}{2}\pi\left(u^2+v^2\right)^2\lambda^3\right\}$ (3^{rd} *order spherical aberration or* C_3)
$\left\{W(4,2), \frac{1}{2}\pi\left(u^2+v^2\right)\lambda^3((u-v)(u+v)\cos(2\phi(4,2))+2uv\sin(2\phi(4,2)))\right\}$
$\left\{W(4,4), \frac{1}{2}\pi\lambda^3\left(\left(u^4-6v^2u^2+v^4\right)\cos(4\phi(4,4))+4u(u-v)v(u+v)\sin(4\phi(4,4))\right)\right\}$
$\left\{W(5,1), \frac{2}{5}\pi\left(u^2+v^2\right)^2\lambda^4(u\cos(\phi(5,1))+v\sin(\phi(5,1)))\right\}$
$\left\{W(5,3), \frac{2}{5}\pi\left(u^2+v^2\right)\lambda^4\left(u\left(u^2-3v^2\right)\cos(3\phi(5,3))-v\left(v^2-3u^2\right)\sin(3\phi(5,3))\right)\right\}$
$\left\{W(5,5), \frac{2}{5}\pi\lambda^4\left(u\left(u^4-10v^2u^2+5v^4\right)\cos(5\phi(5,5))+v\left(5u^4-10v^2u^2+v^4\right)\sin(5\phi(5,5))\right)\right\}$
$\left\{W(6,0), \frac{1}{3}\pi\left(u^2+v^2\right)^3\lambda^5\right\}$ (5^{th} *order spherical aberration or* C_5)
$\left\{W(6,2), \frac{1}{3}\pi\left(u^2+v^2\right)^2\lambda^5((u-v)(u+v)\cos(2\phi(6,2))+2uv\sin(2\phi(6,2)))\right\}$
$\left\{W(6,4), \frac{1}{3}\pi\lambda^5\left(\left(u^6-5v^2u^4-5v^4u^2+v^6\right)\cos(4\phi(6,4))+4uv\left(u^4-v^4\right)\sin(4\phi(6,4))\right)\right\}$
$\left\{W(6,6), \frac{1}{3}\pi\lambda^5\left(\left(u^6-15v^2u^4+15v^4u^2-v^6\right)\cos(6\phi(6,6))+2uv\left(3u^4-10v^2u^2+3v^4\right)\sin(6\phi(6,6))\right)\right\}$

jems describes wave-front aberrations to order 8.

Wave-front aberrations to order 8

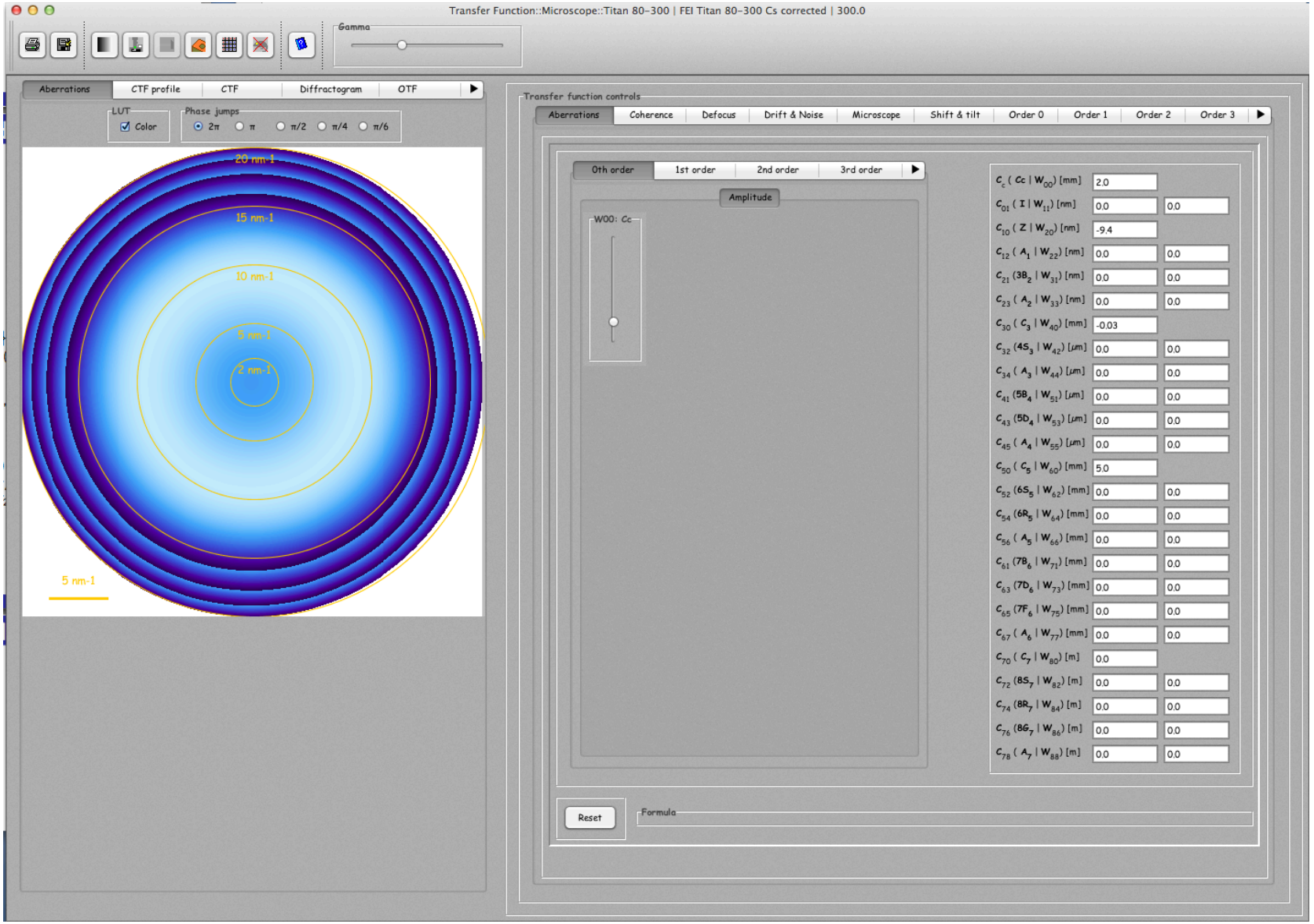

Taking into account partial spatial and temporal coherence

Coherence of illumination:

- Source size (spatial coherence).
- Energy spread (temporal coherence).

Partial coherence (always the case): $\widetilde{T}(q', q)$: transmission cross-coefficients $\Longrightarrow$ is approximated by a transfer function $\widetilde{T}(\vec{u})$ and several envelope functions (attenuation of a range of spatial frequencies)..

Approximations: phase contrast transfer function

For weakly scattering objects (weak phase objects) the imaginary part of the (complex) transfer function, *Phase Contrast Transfer Function*, is only considered and

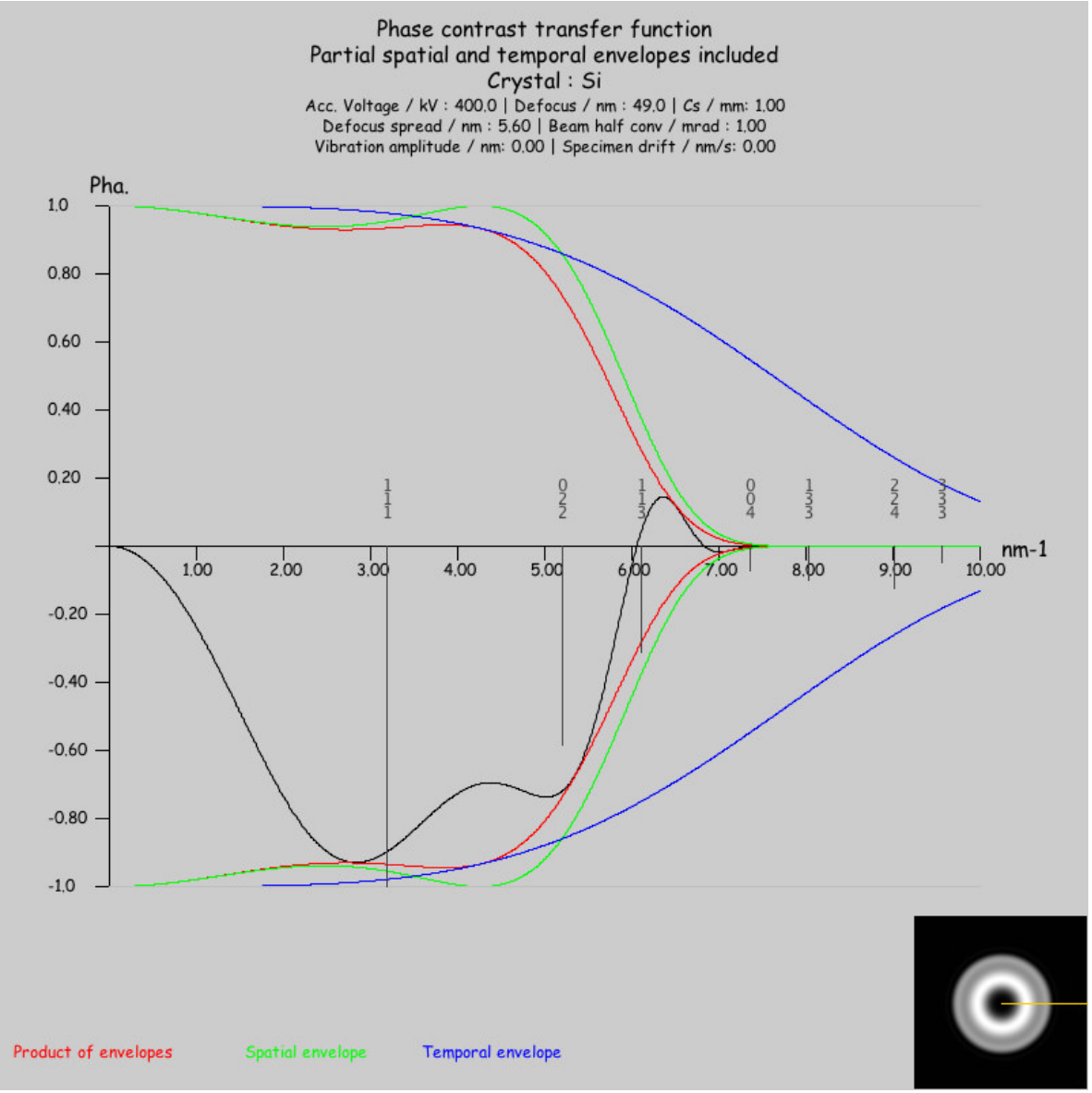

Phase object: change of phase φ

When the crystal potential $V(\vec{r})$ is constant on dz arbitrarily small, the wave-vector of the electron of energy $(e\,(E + V(\vec{r}))$ is:

$$k = \sqrt{\frac{2\,m\,e\,(E + V(\vec{r}))}{h^2}}$$

The refraction index of the media $\vec{n}$ i.e. ratio of the wave-vector of the media to that of vacuum ($|V(\vec{r})| << E$) is:

$$n = \frac{\vec{k_m}}{\vec{k_v}} = \sqrt{\frac{E + V(\vec{r})}{E}} \approx 1 + \frac{V(\vec{r})}{2E}$$

$\Longrightarrow$ Change of phase φ between the wave-function in vacuum and in the crystal for the same distance d$\vec{z}$:

$$\mathrm{d}\varphi = (\vec{k_m} - \vec{k_v}) \cdot \mathrm{d}\vec{r} = (n-1)|\vec{k_v}|\mathrm{d}z = \frac{\chi}{2E} V(\vec{r})\mathrm{d}z$$

where $\chi = |k_v|$.

Phase object: $\Psi_o(\vec{x})$

For an object of thickness Δz, the phase change $\Delta\varphi$ is:

$$\begin{aligned}\Delta\varphi &= \frac{\chi}{2E}\int_z^{z+\Delta z} V(\vec{x};z)\mathrm{d}z \\ &= \frac{\chi}{2E}V_p(\vec{x};z)\Delta z\end{aligned}$$

The transmittance function of the object of thickness Δz is:

$$\begin{aligned}\Psi_o(\vec{x}) &= e^{-2\pi\imath\Delta\varphi} \\ &= e^{-2\pi\imath\frac{\chi}{2E}V_p(\vec{x};z)\Delta z} \\ &= e^{-\imath\sigma V_p(\vec{x};z)\Delta z}\end{aligned}$$

where:

$$\sigma = \frac{\pi\chi}{E} = \frac{\pi}{\lambda E}$$

Weak Phase Object Approximation: WPOA

For a ***Weak Phase Object*** the transmittance is approximated by:

$$\Psi_o(\vec{x}) = e^{-\imath\,\sigma V_p(\vec{x};z)} \approx 1 - i\,\sigma V_p(\vec{x};z)$$

The Fourier transform of the weak phase object, $\widetilde{\Psi}_o(\vec{h})$, in the Back Focal Plane of the objective lens) is:

$$\widetilde{\Psi}_o(\vec{h}) = \delta(\vec{h}) - i\,\sigma\,\widetilde{V}_p(\vec{h};z) \tag{1}$$

Note that $\delta(\vec{h})$, the Fourier transform incident wave-function (plane-wave) and the object information, $\sigma\,\widetilde{V}_p(\vec{h};z)$, are out-of-phase by $\frac{\pi}{2}$. As a consequence interference between the transmitted beam and the reflections is not possible.

Image function: $\widetilde{\Psi}_i(\vec{h})$

$\widetilde{\Psi}_i(\vec{h})$ is the product of microscope's transfer function $\widetilde{T}(\vec{h})$ by the object wave-function $\widetilde{\Psi}_o(\vec{h})$:

$$\begin{aligned}\widetilde{\Psi}_i(\vec{h}) &= \widetilde{\Psi}_o(\vec{h})\,\widetilde{T}(\vec{h}) \\ &= \widetilde{\Psi}_o(\vec{h})\,e^{2\pi\imath\chi(\vec{h})}\end{aligned}$$

where $\chi(\vec{h})$ is given by (Δ_z defocus (W_{20}) and C_s spherical aberration coefficient (W_{40})):

$$\chi(\vec{h}) = \frac{C_s\,\lambda^3\,(\vec{h}\cdot\vec{h})^2}{4} - \frac{\Delta_z\,\lambda(\vec{h}\cdot\vec{h})}{2}$$

Intensity in the mage plane: $I(\vec{x})$

The image wave-function is:

$$\widetilde{\Psi}_i(\vec{h}) = [\delta(\vec{h}) - \imath\sigma\widetilde{V}_p(\vec{h};z)][\cos 2\pi\chi(\vec{h}) + \imath \sin 2\pi\chi(\vec{h})]$$

When $\sin 2\pi\chi(\vec{h}) = -1$ and $\cos 2\pi\chi(\vec{h}) = 0$ for the most important reflections $\vec{h}$, $\widetilde{\Psi}_i(\vec{h})$ becomes:

$$\widetilde{\Psi}_i(\vec{h}) = \delta(\vec{h}) - \sigma\widetilde{V}_p(\vec{h};z)$$

The image intensity $(\Psi_i(\vec{x})\Psi_i^*(\vec{x}))$ is given by:

$$I(\vec{x}) = (1 - \sigma V_p(\vec{x};z))(1 - \sigma V_p(\vec{x};z)) \approx 1 - 2\sigma V_p(\vec{x};z)$$

WPOA image formation summary

The image intensity of a weak phase object:

- Intensityé is linearly related to the projected potential.
- Intensity shows dark dots where the projected potential is important (at the atomic columns positions).
- Intensity shows white dots where the projected potential is null (at the channel positions).

Remark: on aberrations corrected microscopes it is possible acquire images with slightly negative C_s and have:

$$I(\vec{x}) \approx \sigma V_p(\vec{x}; z)$$

Weak phase object: inverse contrast

When $\sin 2\pi\,\chi(\vec{h}) = 0$ et $\cos 2\pi\,\chi(\vec{h}) = 1$, the image intensity $(\Psi_i(\vec{x})\Psi_i^*(\vec{x}))$ becomes since:

$$\widetilde{\Psi}_i(\vec{h}) = [\delta(\vec{h}) - \imath\,\sigma\,\widetilde{V}_p(\vec{h}; z)]$$

$$\begin{aligned} I(\vec{x}) &= (1 - \imath\,\sigma\,V_p(\vec{x}; z))(1 + \imath\,\sigma V_p(\vec{x}; z)) \\ &= 1 + \sigma^2\,V_p^2(\vec{x}; z) \end{aligned}$$

HRTEM image depends on specimen thickness and object defocus

Thickness series

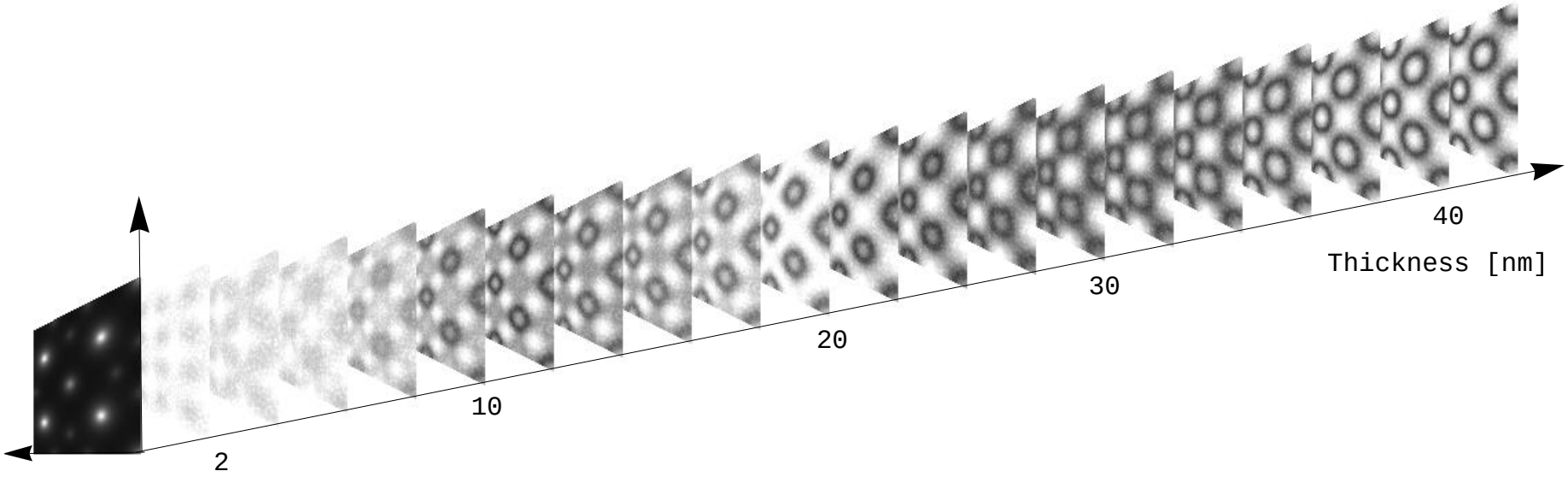

Defocus series

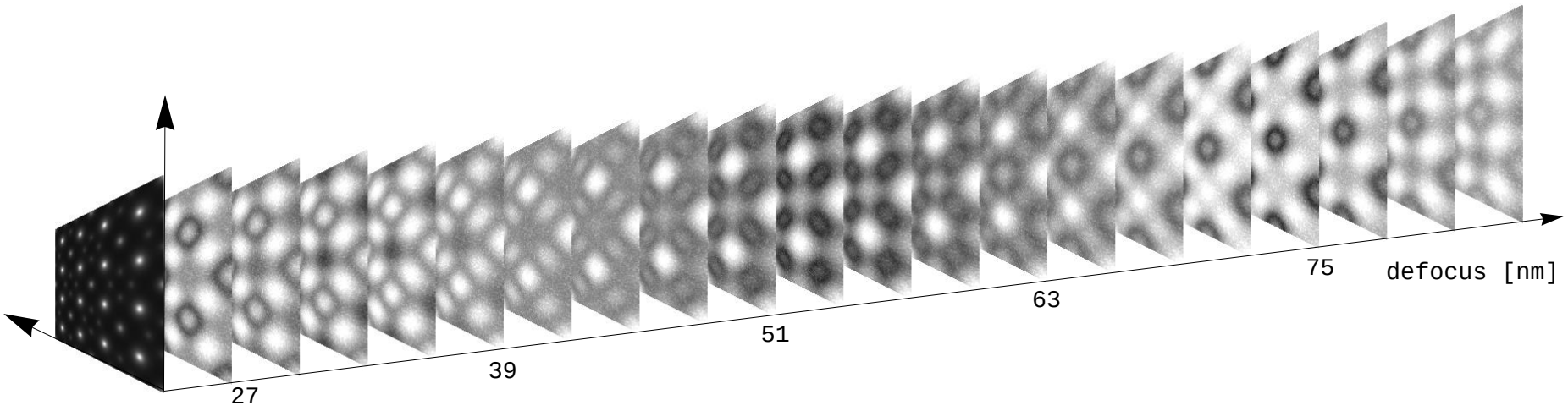

Problems

Problems...

- Object
  - → Atomic scattering amplitude below 50 kV?
  - → Potential by DFT calculation?
  - ...
- HRTEM → Phase of diffracted beams evolves with specimen thickness.
- HRTEM → MTF of image acquisition system (Stobbs factor?).
- HRTEM / HRSTEM → Electron channeling depends on atomic column content.
- HRTEM / HRSTEM → Aberrations of optical system.
- HRTEM → Inelastic scattering (J.M. Cowley, E.J. Kirkland, D. van Dyck, A. Rosenaurer, K. Ishizuka, Z.L. Wang, H. Rose, H. Mueller, L. Allen, ...).
- HRTEM / HRSTEM → Drift, vibration, Johnson-Nyquist noise[11], ...
- ...

[11] S. Uhlemann, H. Mueller, P. Hartel, J. Zach & M. Haider, Phys. Rev. Lett. **111** (2013) 046101.

HRTEM problem: amplitude and phase of diffracted beams

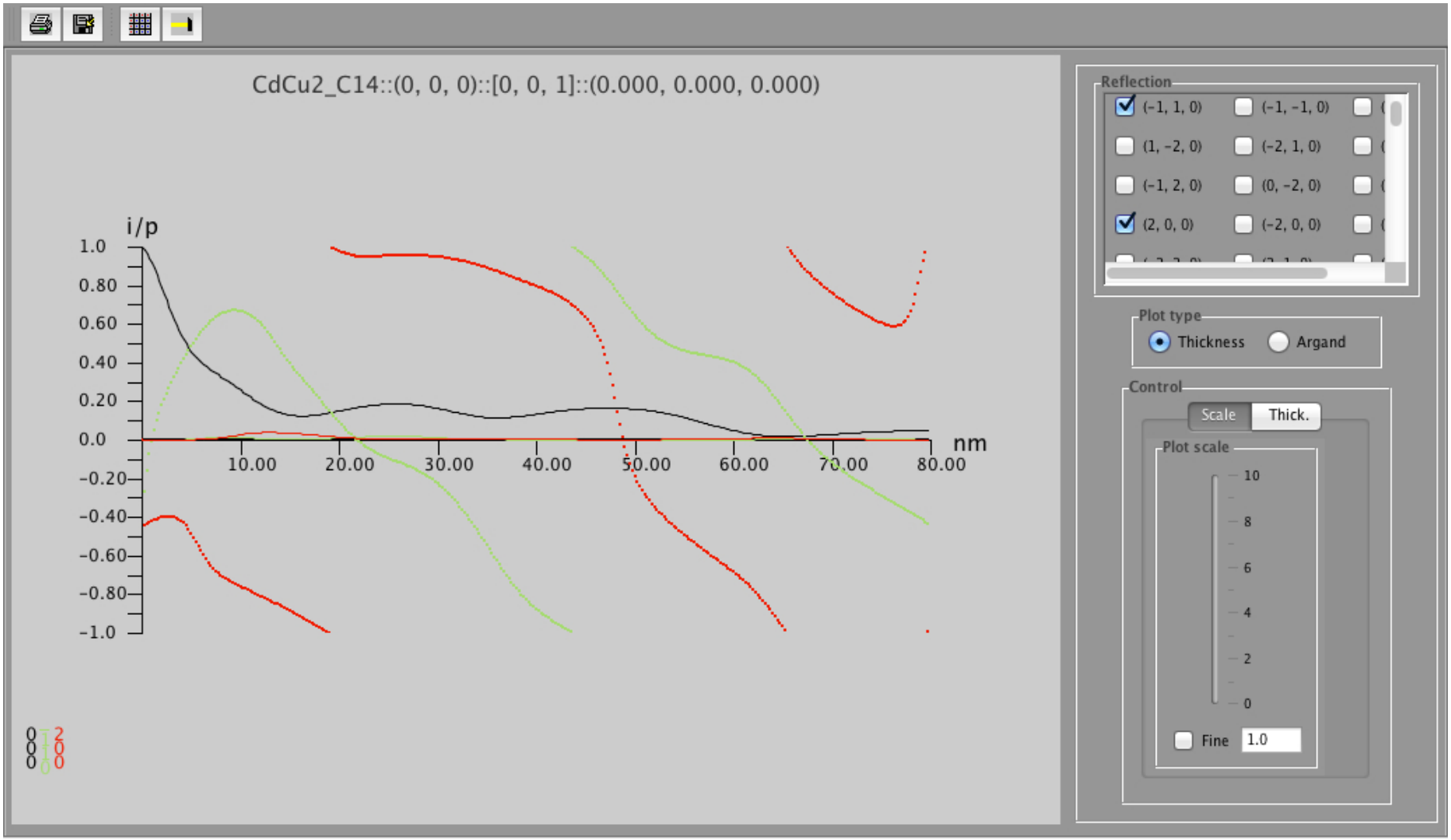

Note that phase of diffracted beam is $\frac{\pi}{2}$ out-of-phase with respect to transmitted beam. As a consequence of the phase change of the reflections, the contrast of the HRTEM images shows fast changes or even contrast reversal with an increase of the specimen thickness.

HRTEM problem: CCD MTF (Gatan MSC 1K x 1K, 24 μm)

To make quantitative comparison with experimental HRTEM images the MTF of the detector must be introduced in the simulation.

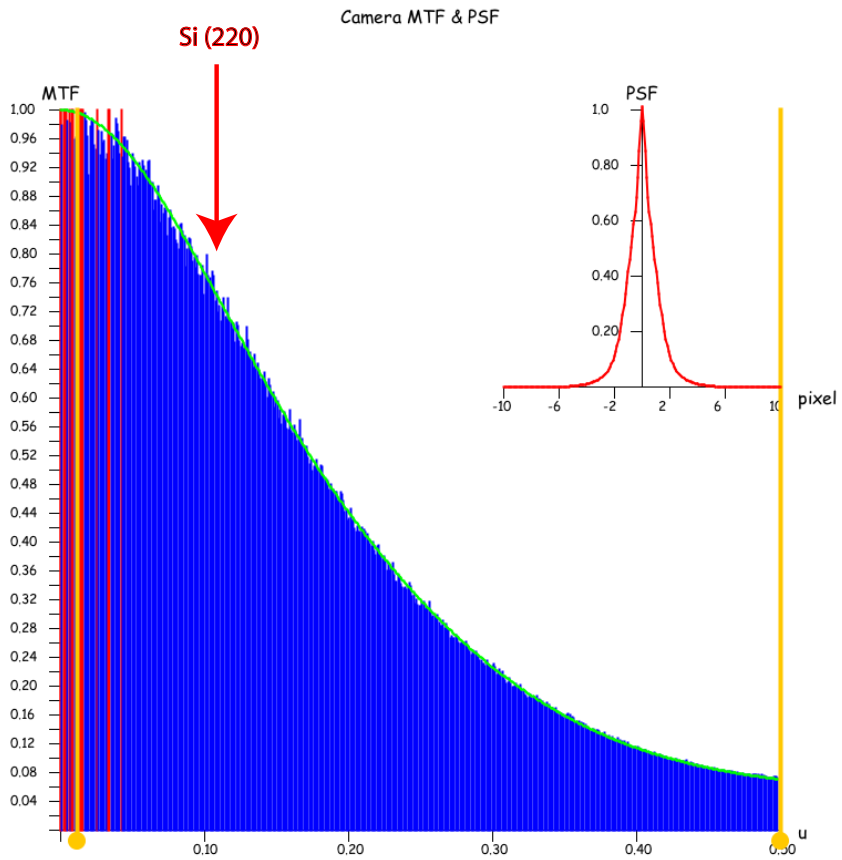

Figure: At high magnification Si (220) planes imaged with high contrast.

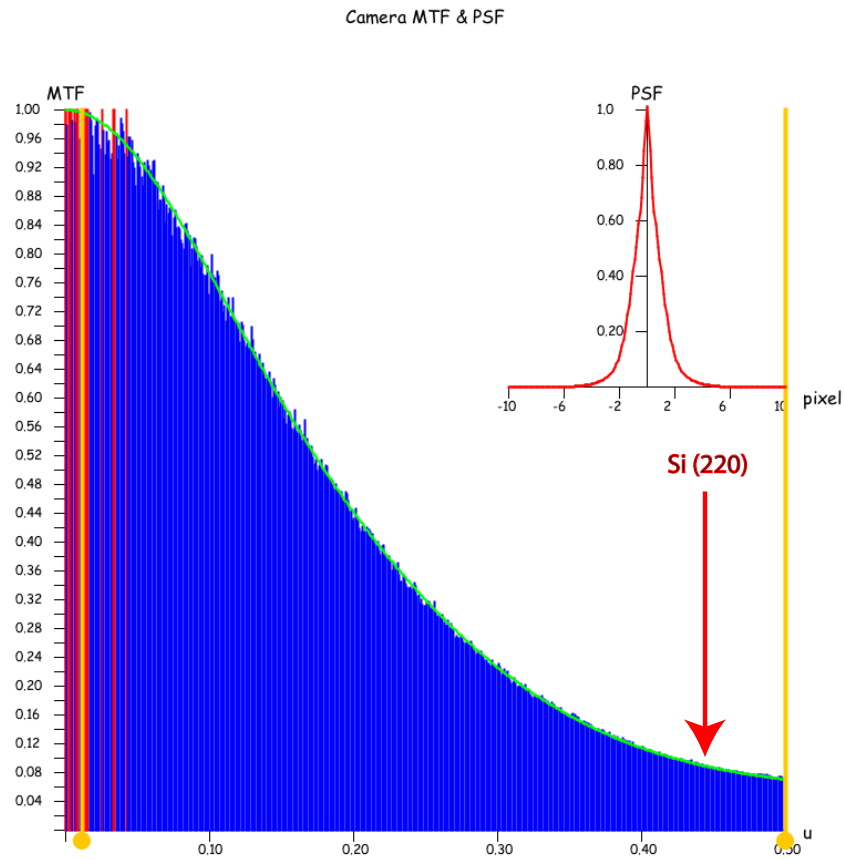

Figure: At low magnification Si (220) planes imaged with low contrast.

For quantitative comparison always use highest possible magnification (or include CCD MTF in simulations)!

CCD MTF: high magnification (900 kx)

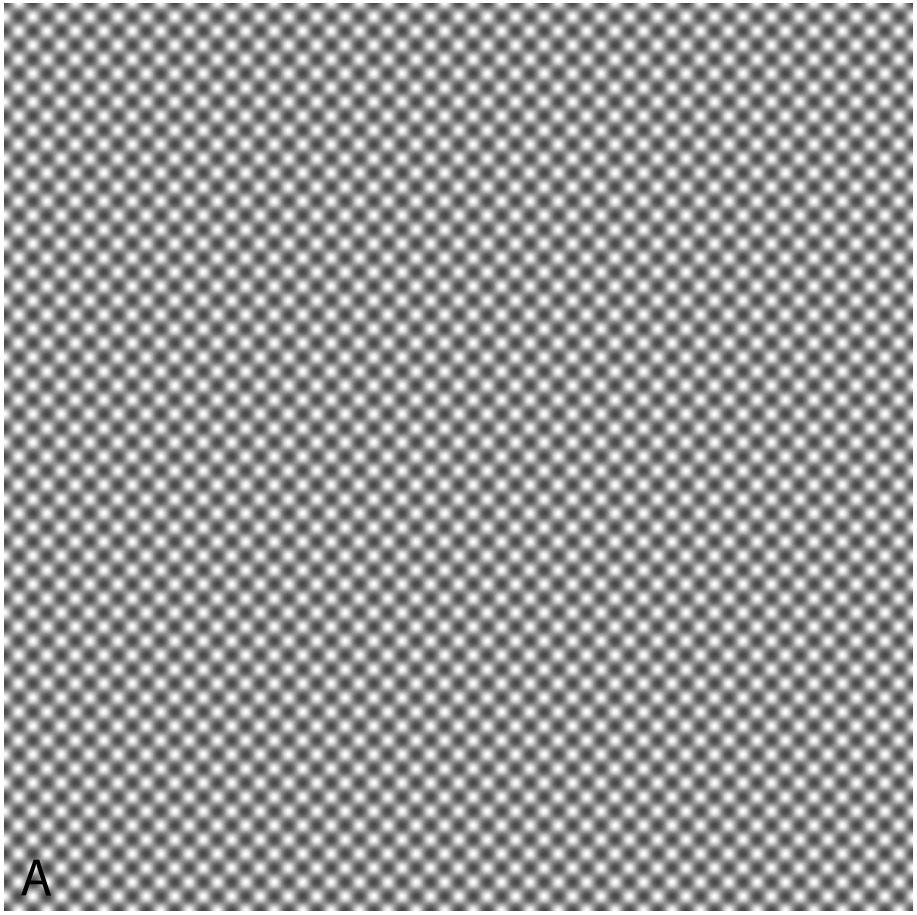

Figure: A: Si [001] simulation.

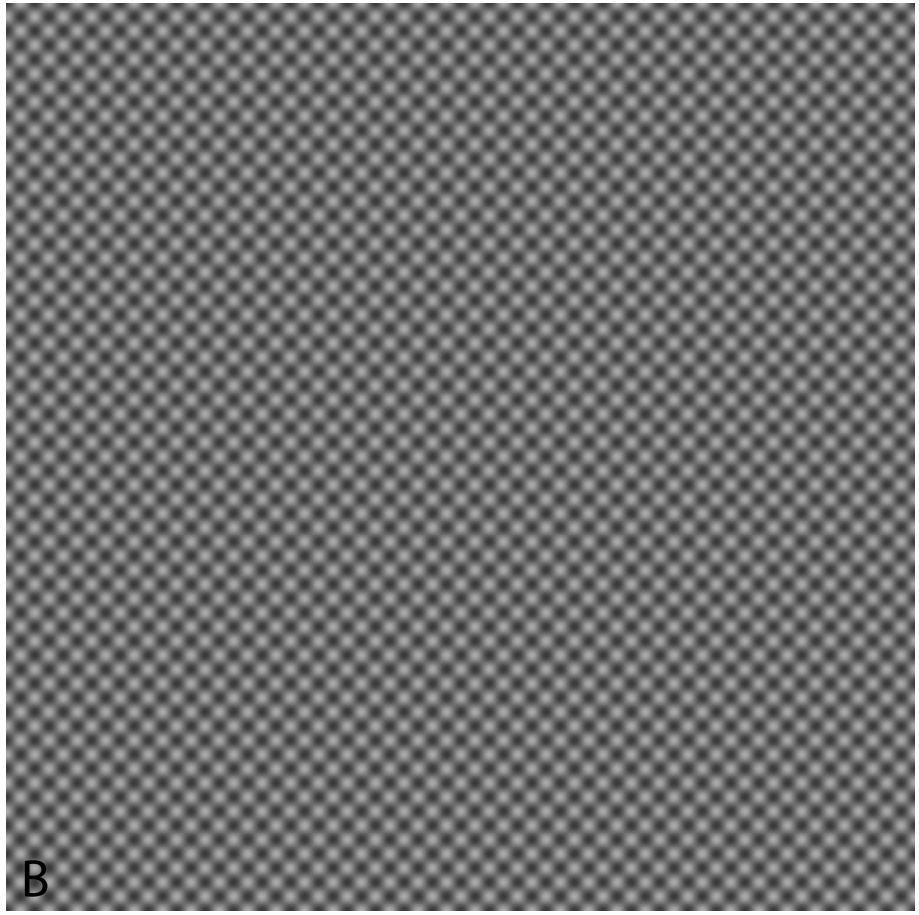

Figure: B: Si [001], simulation + CCD MTF.

CCD MTF: low magnification (225 kx)

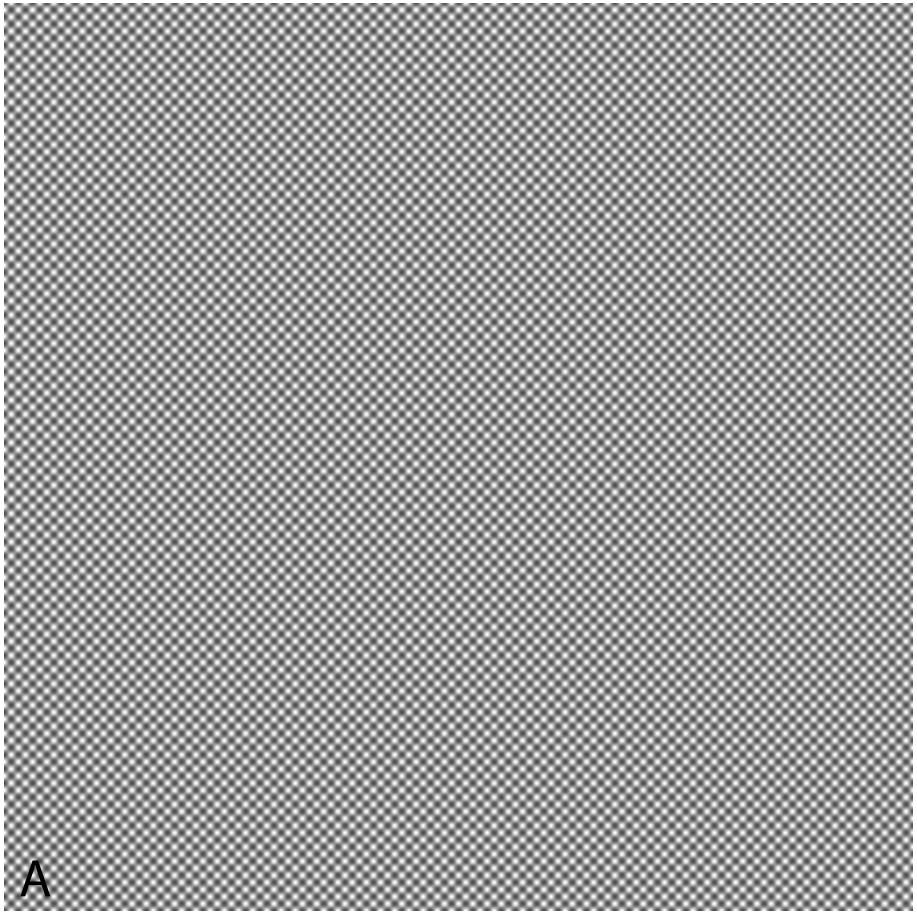

Figure: A: Si [001] simulation.

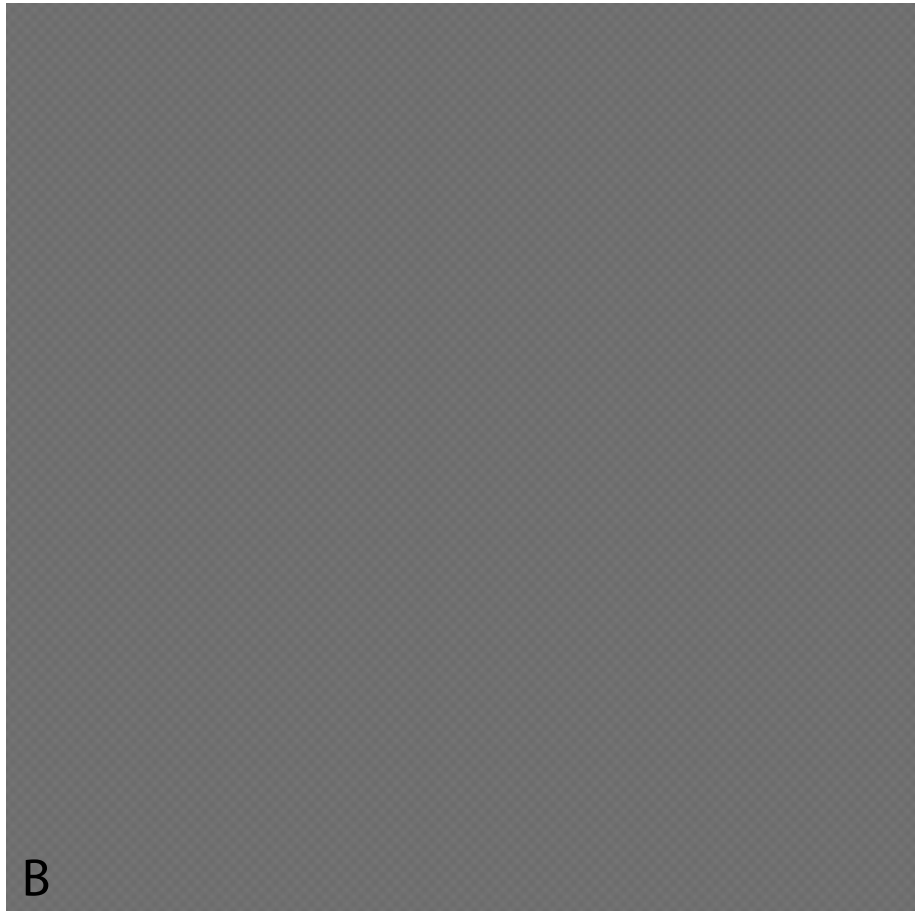

Figure: B: Si [001], simulation + CCD MTF.

Does C_s and C_c correction solves all imaging problems?

Example: CdCu_2, visibility of the 3 Cu atomic columns.

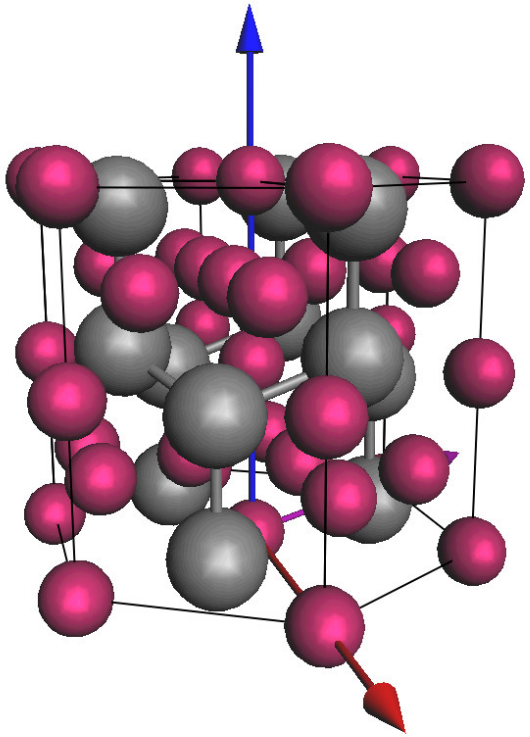

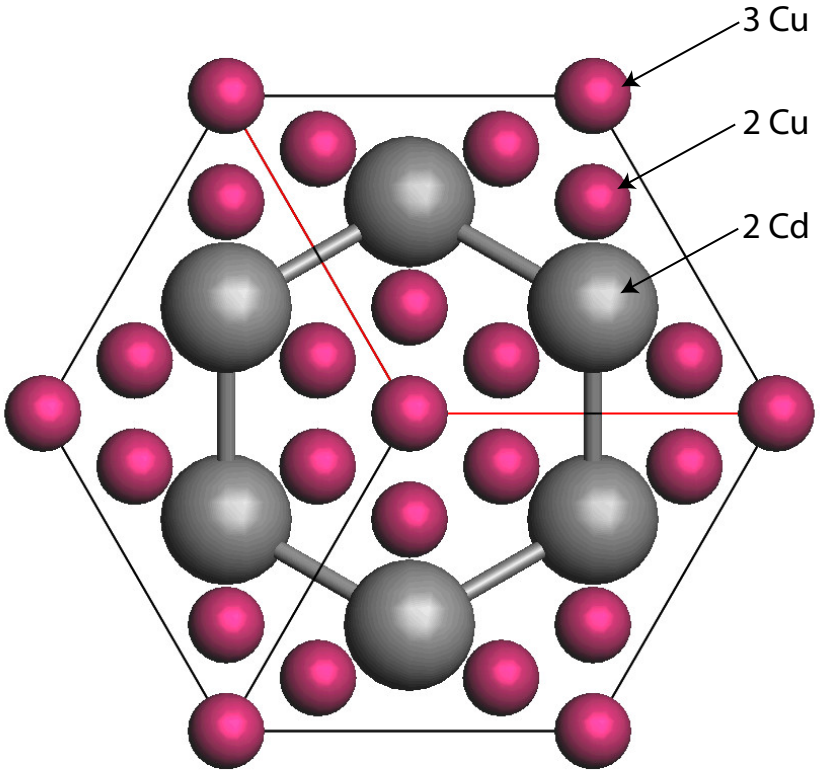

HRTEM image simulation conditions

Acc. [kV]	$C_s[mm]$	$C_5[mm]$	$C_c[mm]$	$\Delta E[eV]$	Z [nm]	$\Delta z[nm]$
300	-0.008	30	0.5	0.6	-4.9	1
300	-0.008	30	0.1	0.2	-2.0	1

Dynamical scattering effects are not affected by C_s and/or C_c corrected TEM!

$CdCu_2[001]$: imaging parameters set 1

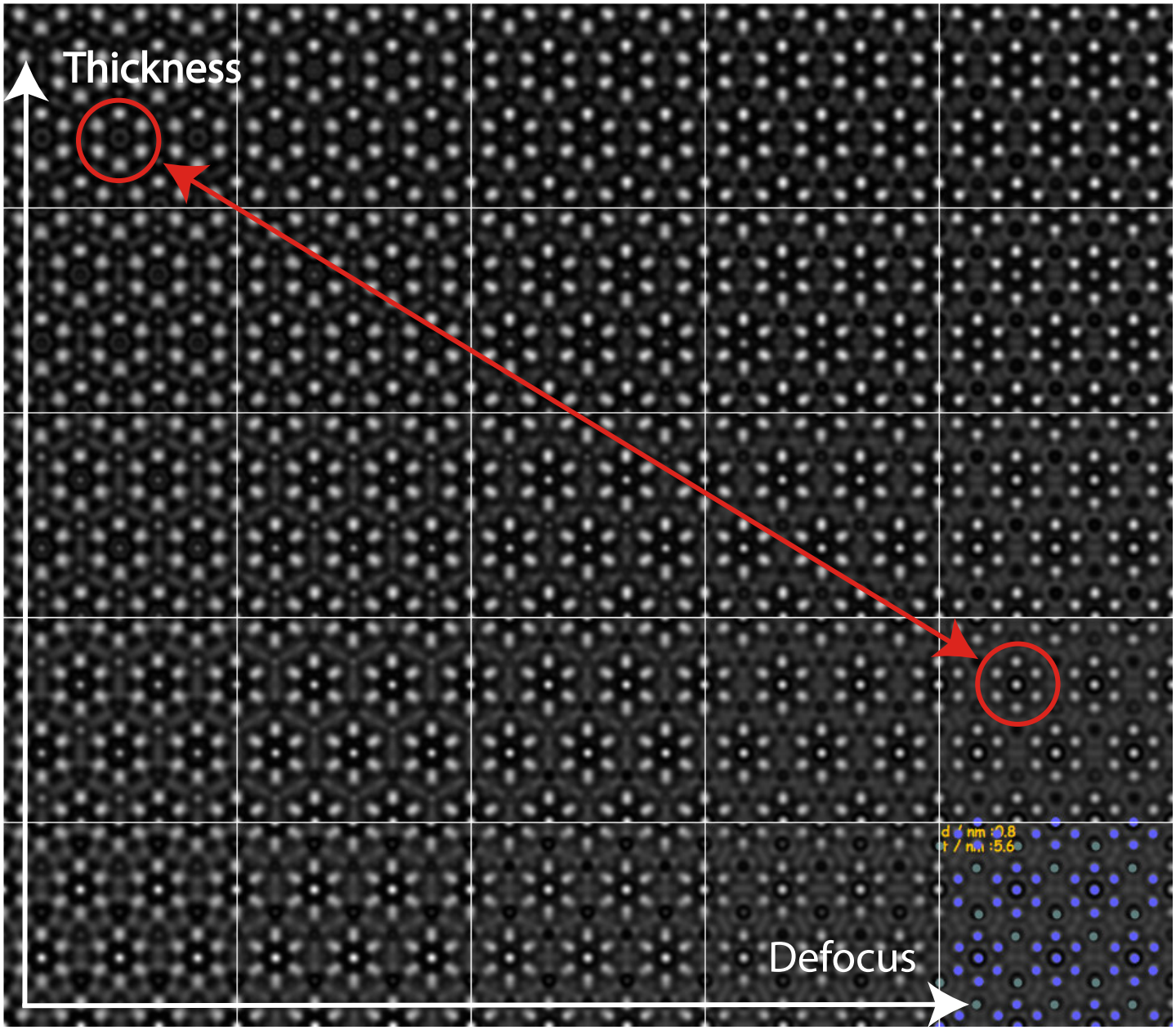

Visibility of 3 Cu atomic columns depends on specimen thickness and defocus.

$CdCu_2[001]$: imaging parameters set 2

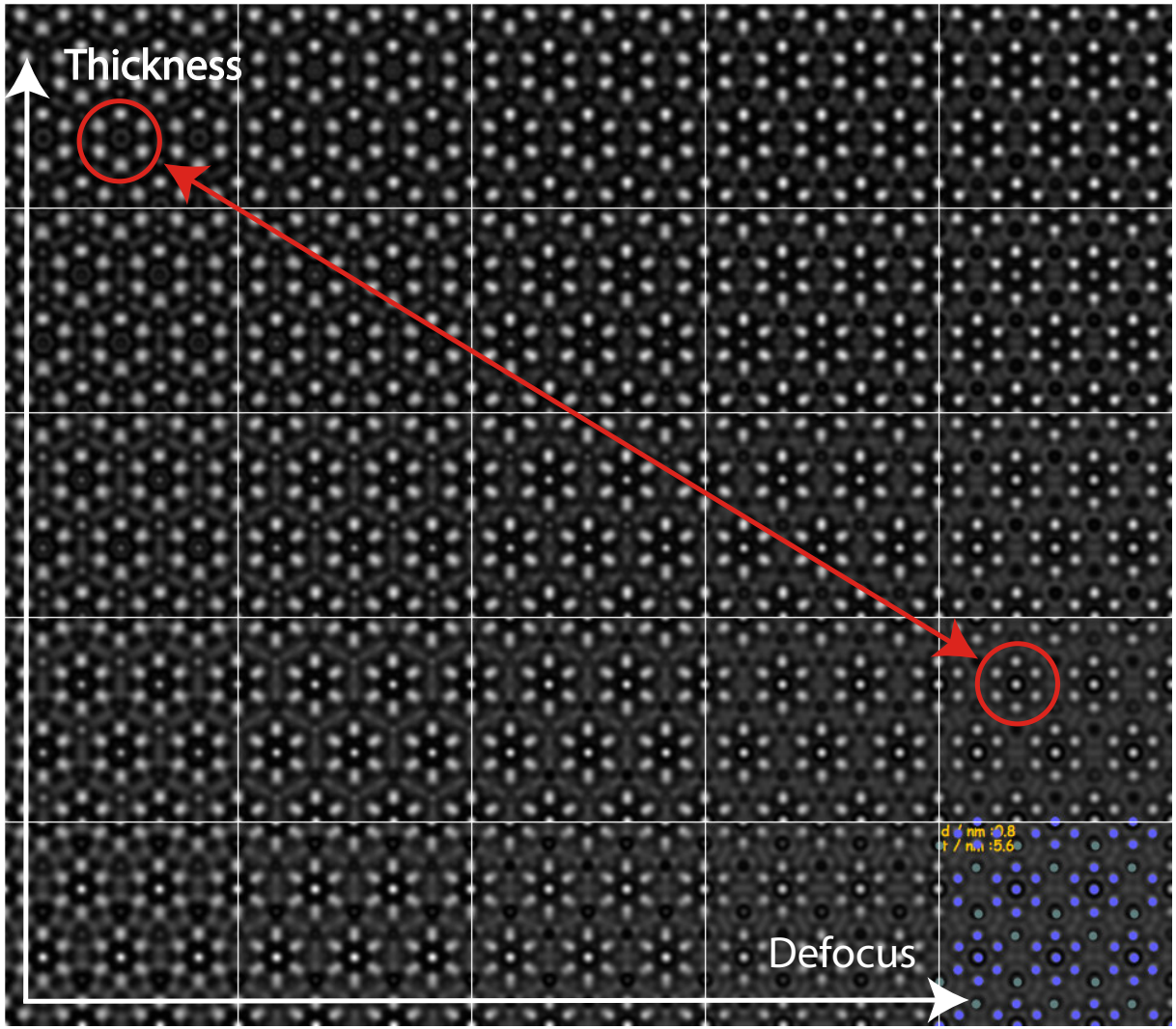

Improving C_c and ΔE does not affect the visibility of 3 the Cu atomic columns. It depends on specimen thickness (and defocus indeed). Visibility of the 3 Cu atomic columns is always affected by dynamical scattering. Only extremely thin specimen ($\leq$ 10 nm) will allow faithful imaging of crystal projected potential.

HRTEM or STEM HAADF imaging

High Angle Annular Dark Field (HAADF): inelastically scattered electrons.
When simulation is necessary how to simulate images?
Numerous approximations:

- Simple projected + convolution with probe intensity: no channeling effect (Weak Object Approximation).
- Multislice calculation: channeling + inelastic scattering (absorption potential) + convolution with probe intensity.
- Frozen lattice (phonon) approximation: atoms of super-cell displaced out of equilibrium position, probe scanned on imaged area, intensity collected by annular detector.
- Pennycook, Nellist, Ishizuka, Shiojiri, Allen, Wang, Rosenauer, van Dyck, ...

Except the first 2 methods, simulation time expensive (luxury?). Approximations (necessity) may suffice...

HAADF: graphene

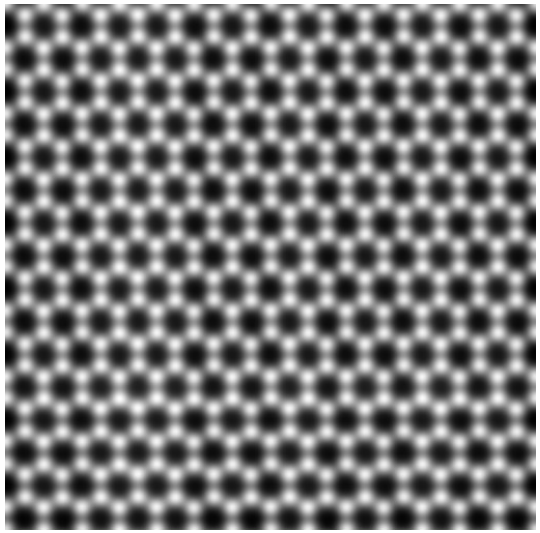

Figure: Proj. pot. approx.

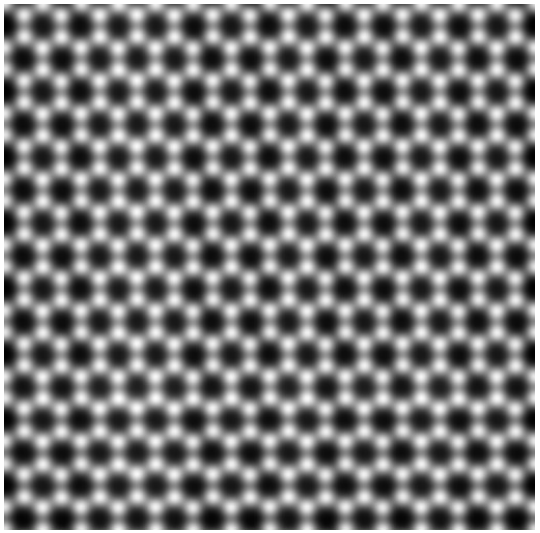

Figure: Channeling calculation.

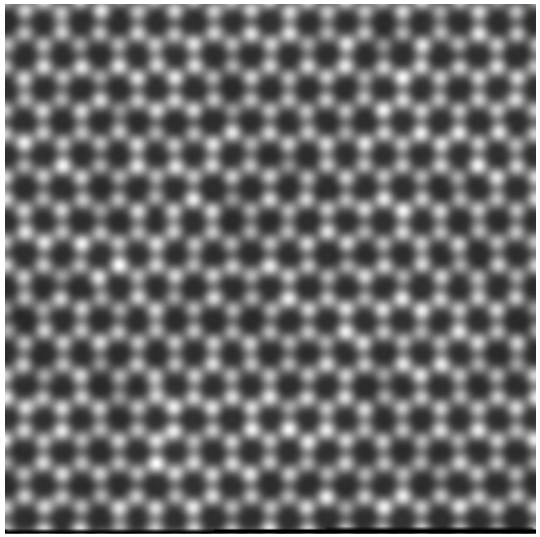

Figure: Frozen lattice 5 conf.

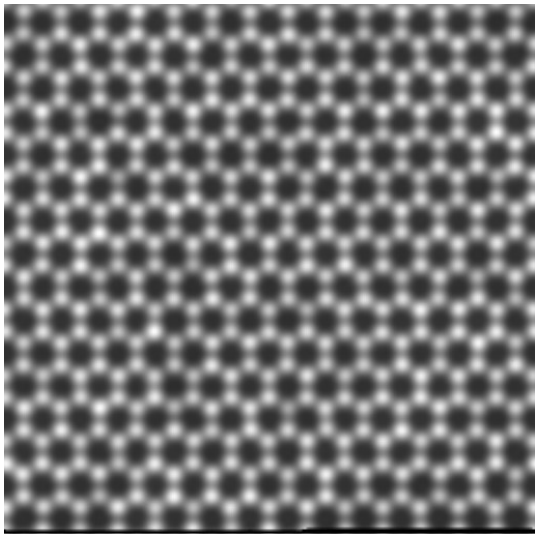

Figure: Frozen lattice 10 conf.

HRSTEM - HRTEM comparison: graphene with add atoms

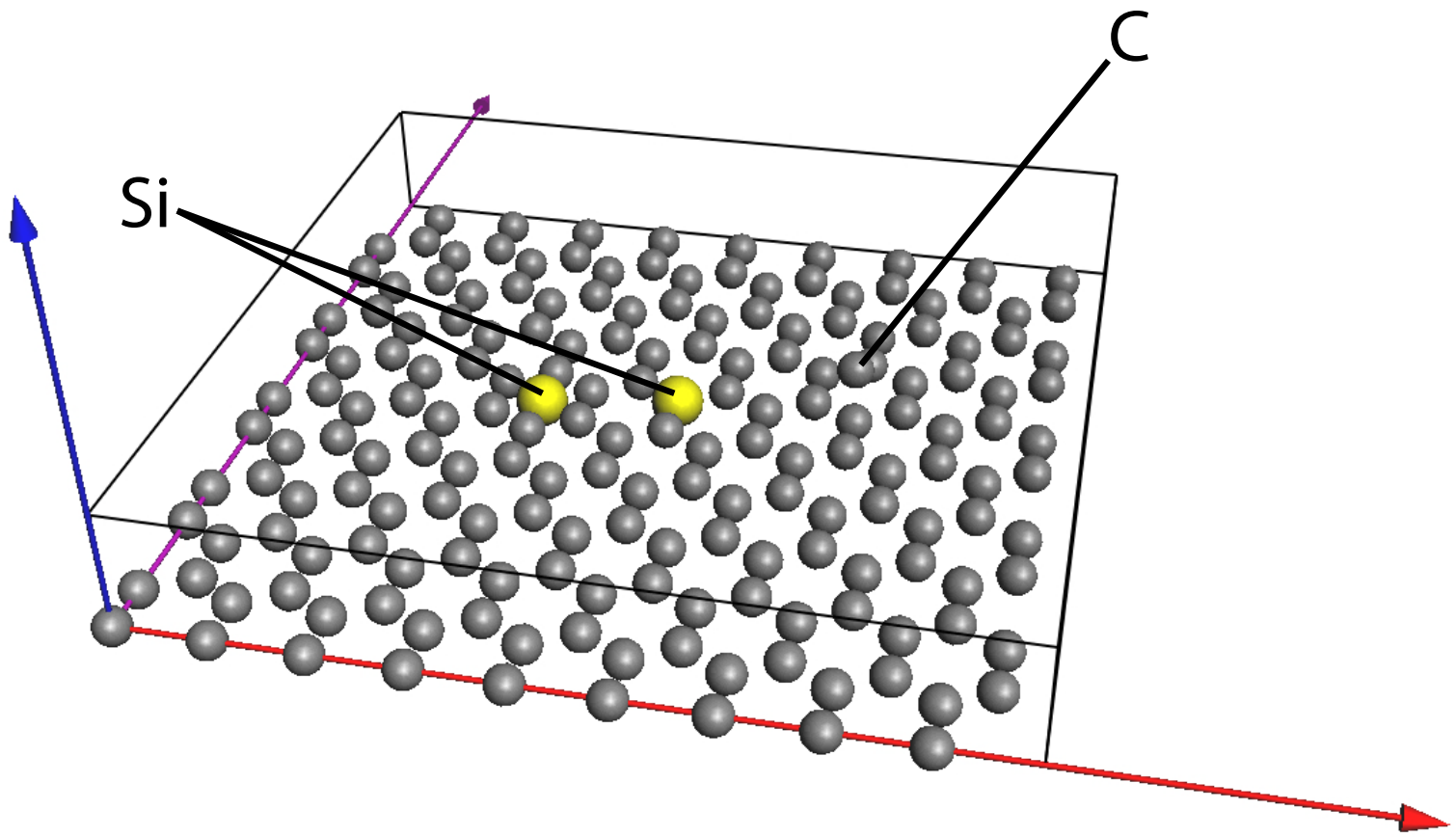

Figure: Graphene with Si in 6 C ring, Si substitutional and 2 C column.

Graphene HAADF (100 kV, 70 -150 mrad)

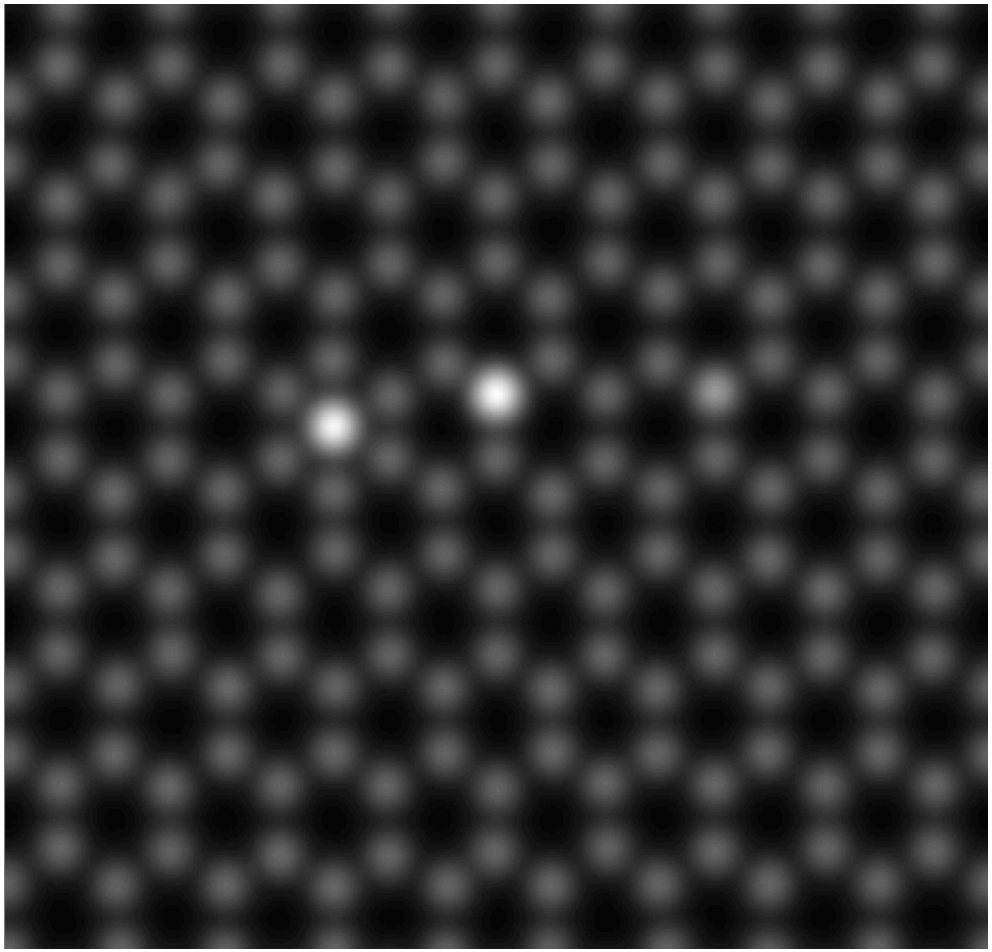

Figure: Frozen lattice (∼400 s).

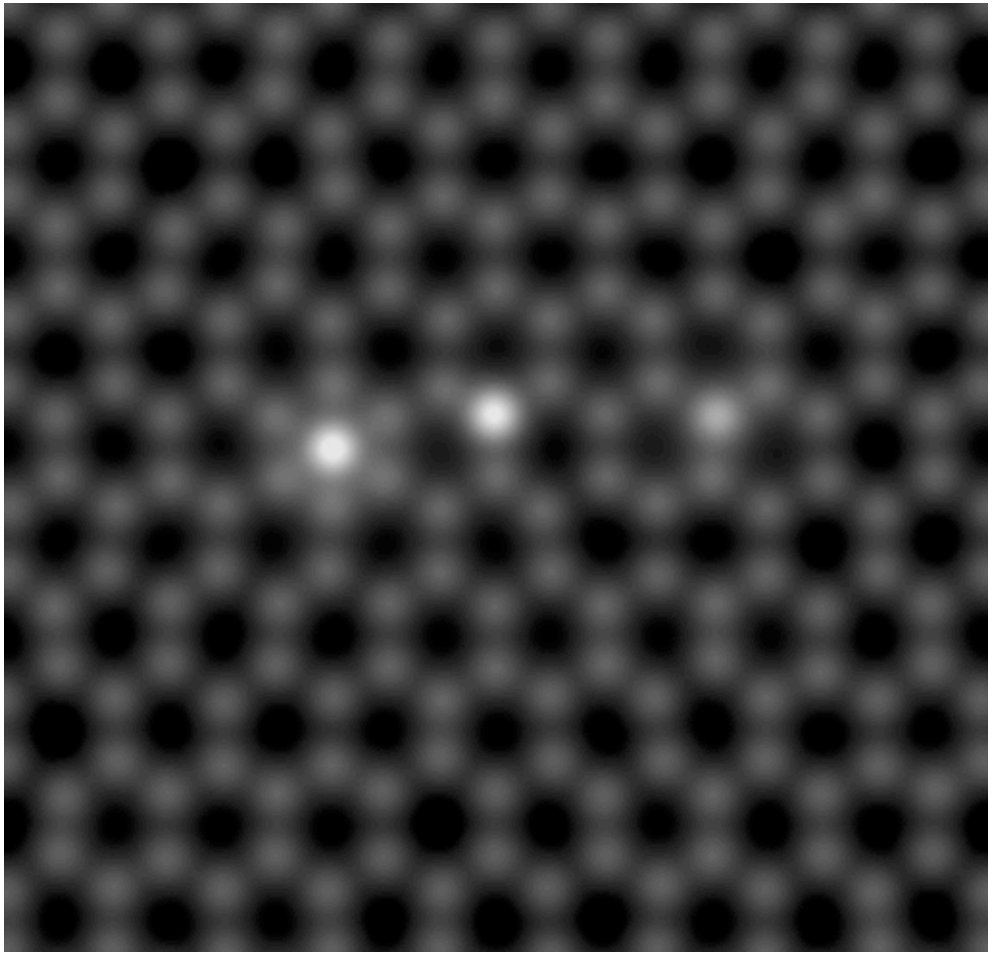

Figure: Channeling (∼2 s).

One Si shows more contrast than 2 C atoms (i $\sim Z^2$) : 14^2 compared to $\sim 2 \times 6^2$.

Graphene HRTEM (100 kV, $C_s - 0.033mm$)

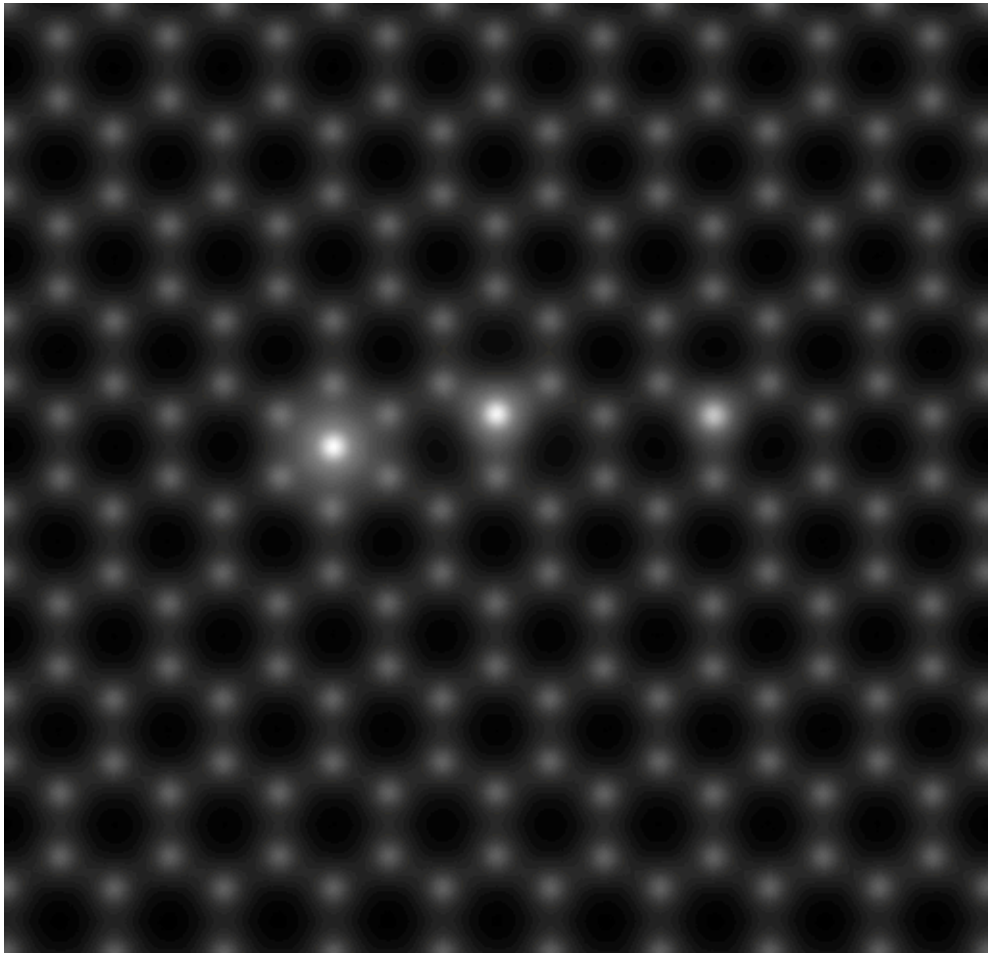

Figure: Weak phase object app., $C_c = 0.5mm$

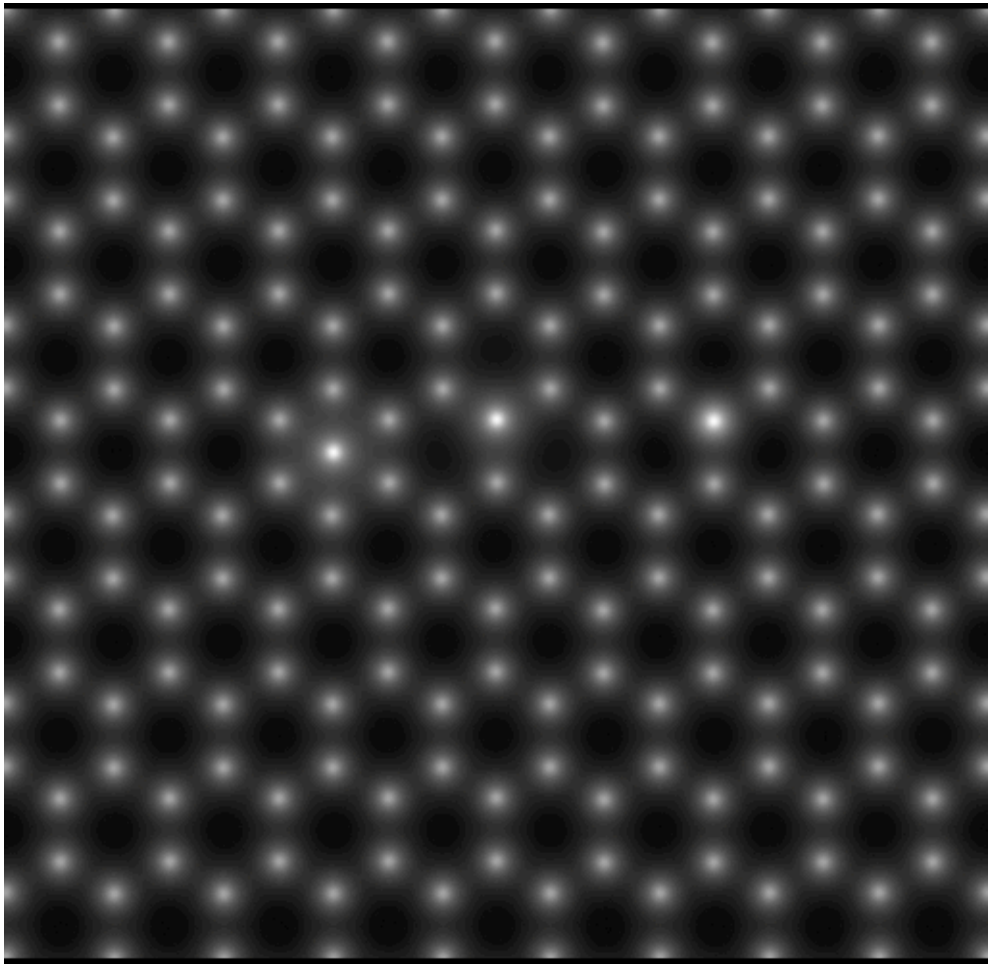

Figure: Multislice, $C_s = -0.033mm$, $C_c = 0$, no thermal magnetic noise.

HRTEM does not display the strong contrast difference between one Si and two C as given by HAADF.

HRTEM / HRSTEM problem: aberrations of optical system

Reaching 0.05 nm resolution sets very strong conditions on aberrations correction.

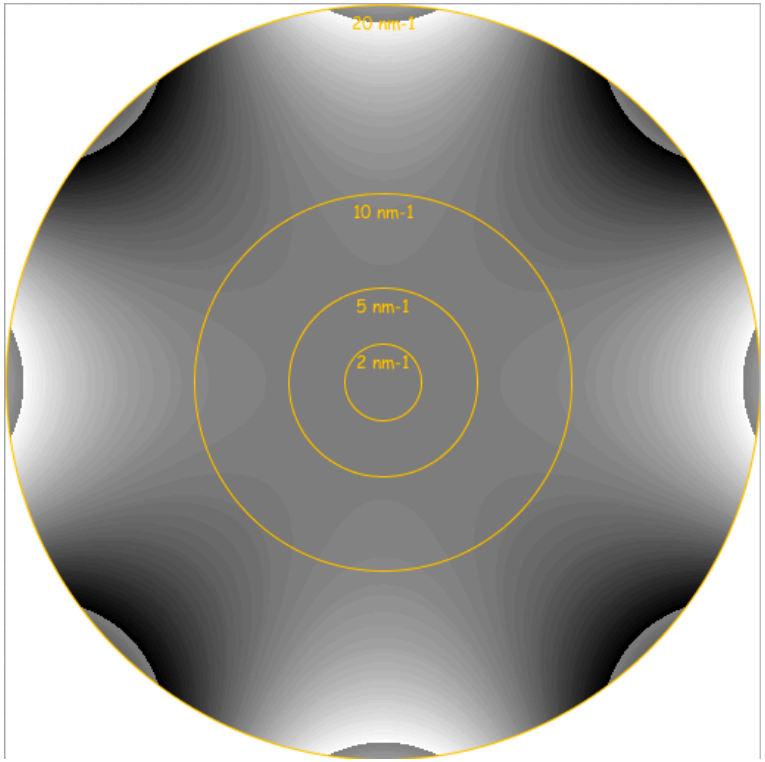

Figure: Aberration figure of $C_{34}(0.5\mu\text{m})$, phase jump at $\frac{\pi}{4}$.

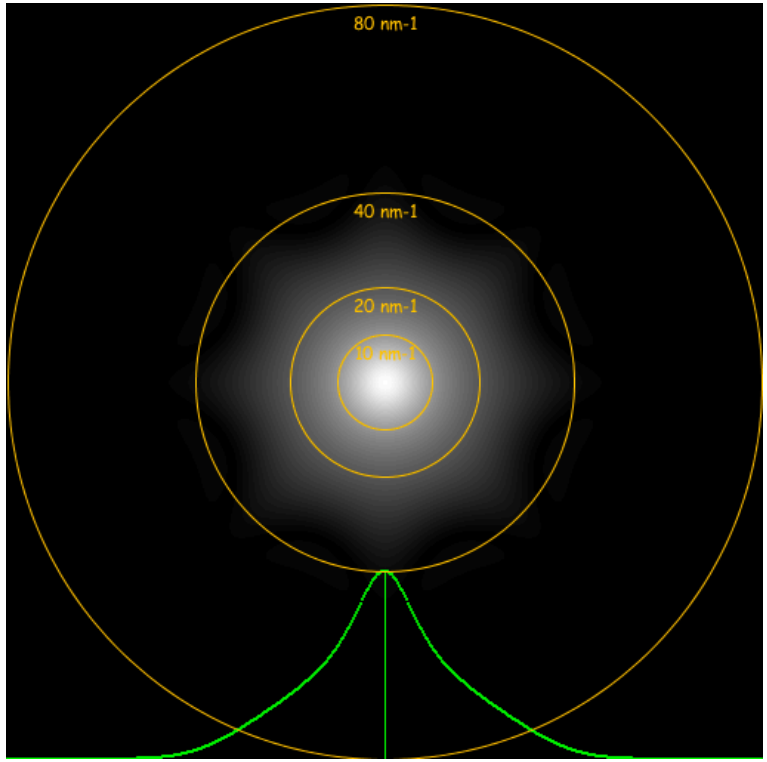

Figure: Optical Transfer Function.

Note that Optical Transfer Function (HRSTEM) transfers higher spatial frequencies than Ccoherent Transfer Function (HRTEM).

HAADF: graphene

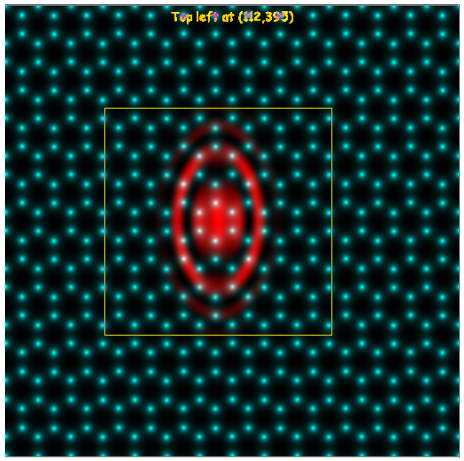

Figure: Probe affected by 2 fold astigmatism.

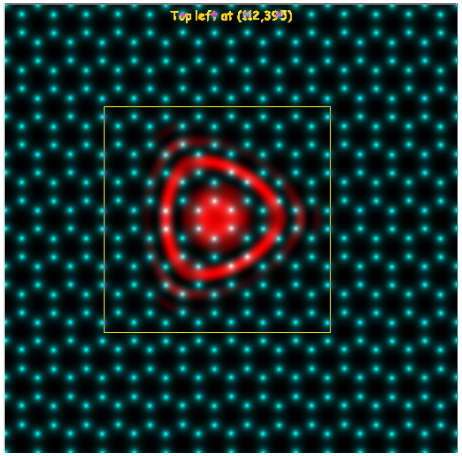

Figure: Probe affected by 3 fold astigmatism.

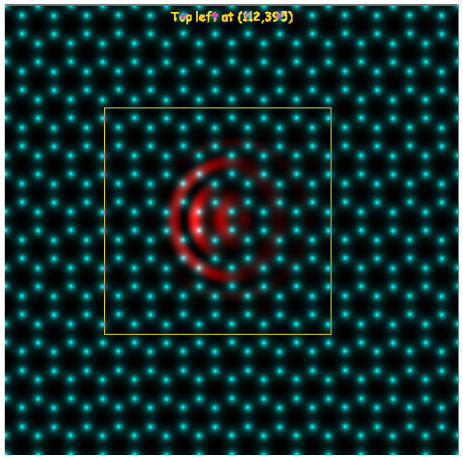

Figure: Probe affected by coma.

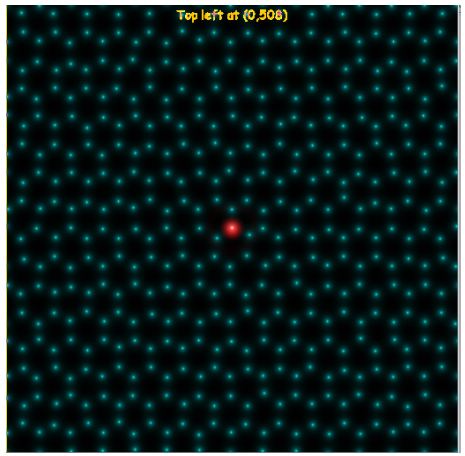

Figure: Corrected probe (best defocus).

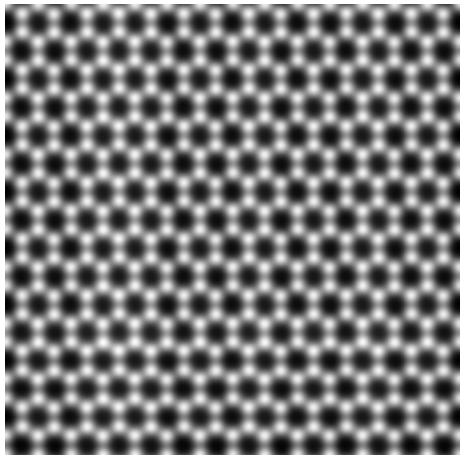

Figure: HAADF projected potential approximation.

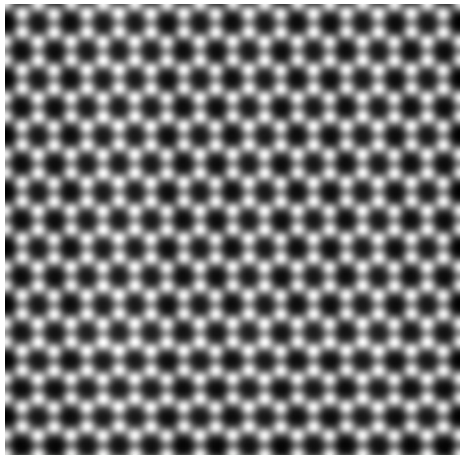

Figure: HAADF multislice calculation (simple).

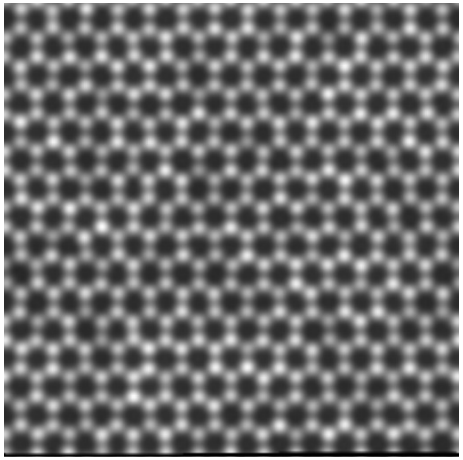

Figure: Frozen phonons 5 configurations.

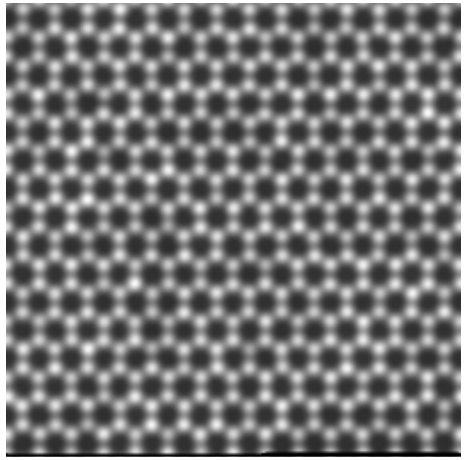

Figure: Frozen phonons 10 configurations.

The two most employed diffraction calculation methods

All approximations are numerically equivalent, but perform best in particular cases.
We will consider only 2 approximations:

- The multislice approximation[12].
- The Bloch-wave method[13].

The multislice method performs best when simulating crystalline or amorphous solids of large unit cell or containing defects while the Bloch-wave method is adapted to the calculation of crystalline solids of small unit cell and in any [uvw] orientation. The Bloch-wave method has also several advantages (speed, ease of use) for simulating CBED, LACBED or PED patterns and for polarity and chirality determination.

[12] J. Cowley and A.F. Moodie, Proc. Phys. Soc. B70 (1957) 486, 497 and 505.
[13] H. A. Bethe, Ann. Phys. 87 (1928), 55.

Multislice method

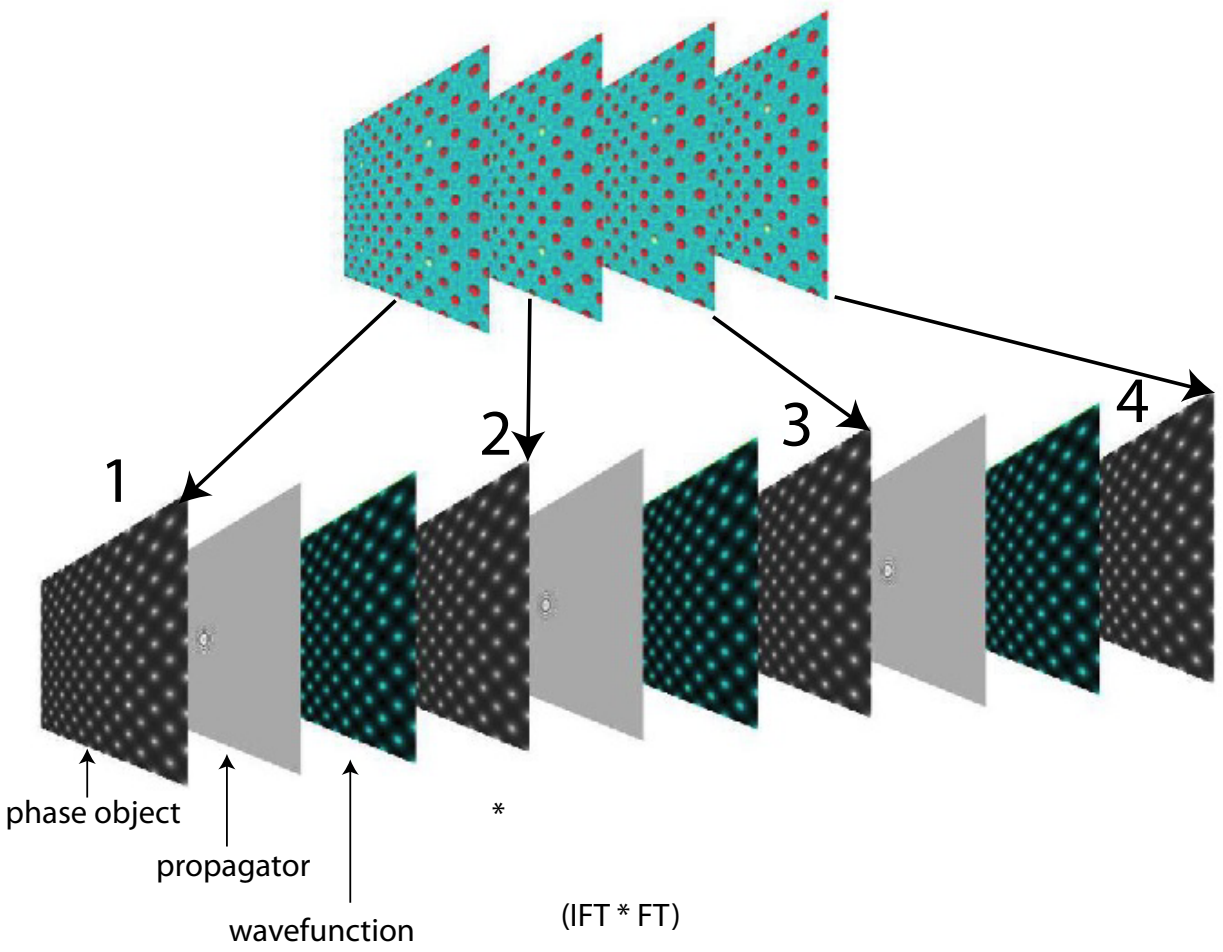

The solid is sliced into thin sub-slices. The incident wave-function is transferred by the first slice (diffraction) and propagated to the next one. The propagation is done within the Fresnel approximation, the distance between the slices being 20 - 50 times the wavelength.

$$\Psi(i+1) = [\Psi(i)PO(i)] \otimes FP_{i \to i+1}$$

Multislice algorithm

2 steps:

- Diffractor: transfer by one slice $\Rightarrow$ multiplication by phase object function ($POF(\vec{\rho})$).
- Propagator: propagation between slices $\Rightarrow$ convolution by the Fresnel propagator (is nowadays performed by a FFT followed by a multiplication and an inverse FFT (FT^{-1}, multiplication, FFT)) (calculation error $O(z)$).

For improved multislice calculations ($O(z^2)$) the wave-function is propagated over $z/2$, then multiplied by the phase-object function of the slice and finally propagated again over $z/2$. Slices do not need to have equal thicknesses.

Work best to simulate:

- Perfects crystals of large unit cell parameters[14].
- Defects under the periodic continuation assumption[15].

Is also used for:

- ADF image simulation in the "Frozen Lattice" approximation[16].

[14] K. Ishizuka, Acta Cryst. A33 (1977) 740-749.

[15] A.J. Skarnulis, Thesis, Arizona State University 1975.

[16] E.J. Kirkland, *Advanced Computing in Electron ¡microscopy.*

Multislice: periodic continuation

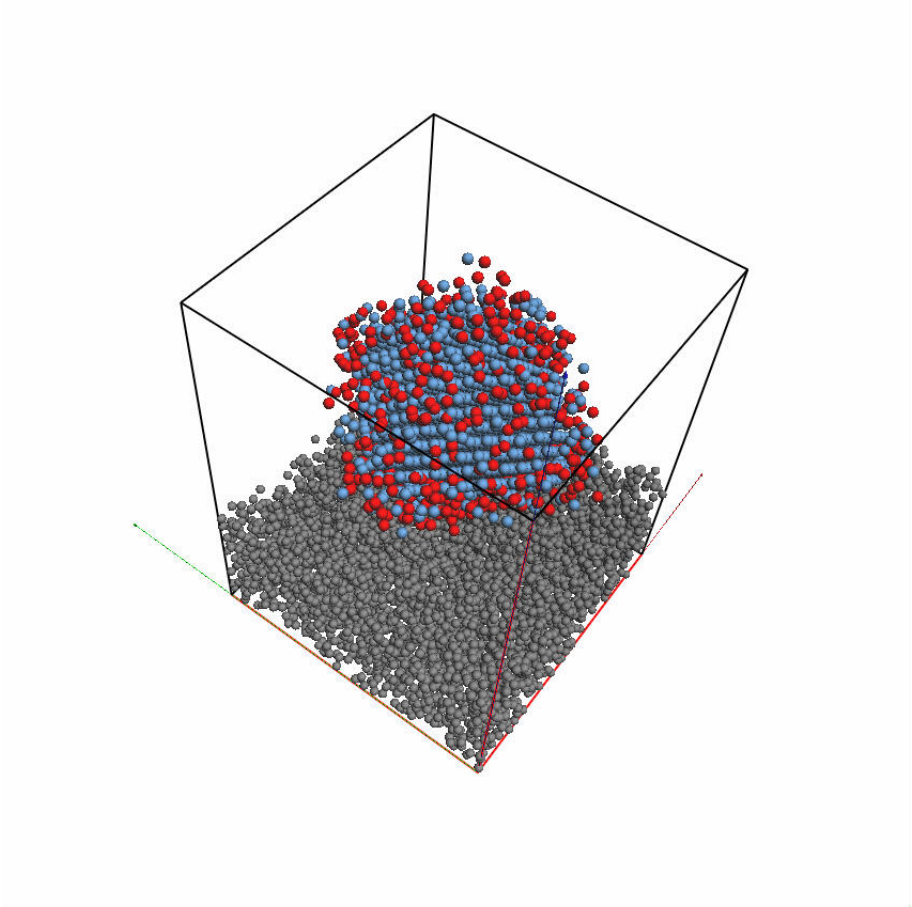

One unit cell model.

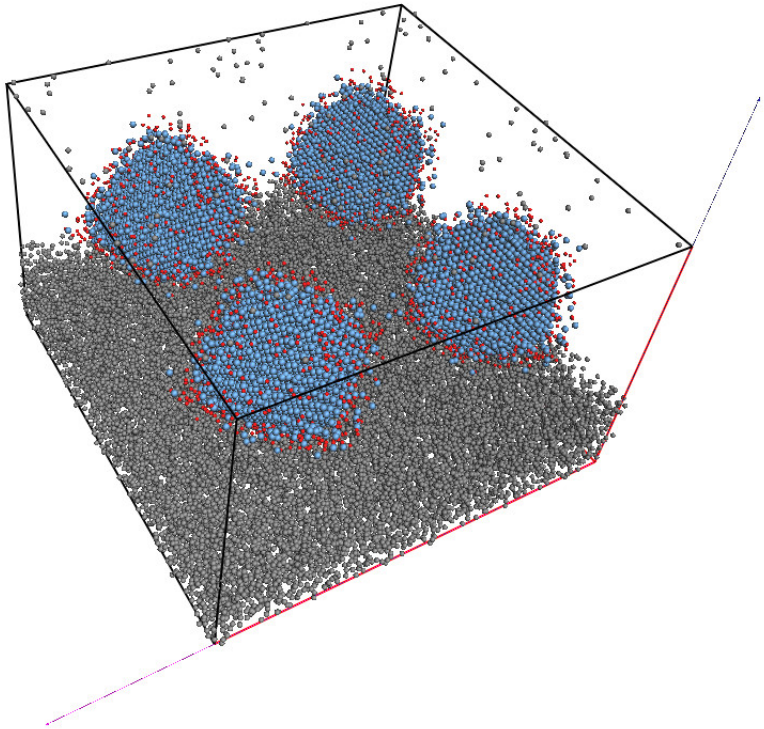

Periodic continuation model (2 x 2 unit cells).

In order to avoid "aliasing problems" during the multislice iterations the phase-object function and the propagator function must be sampled properly and also be "band-limited".

Example multislice: Pt catalyst

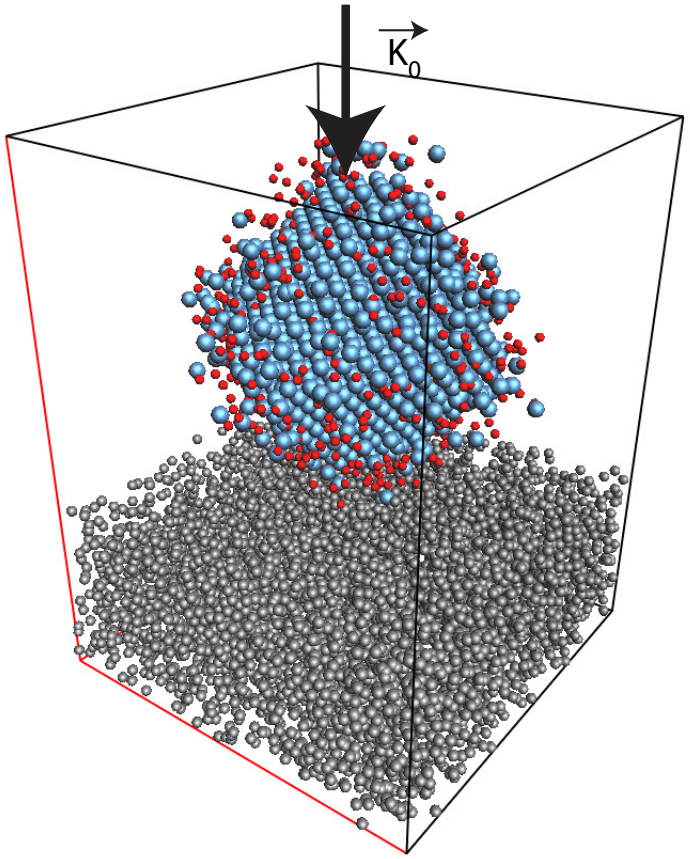

A

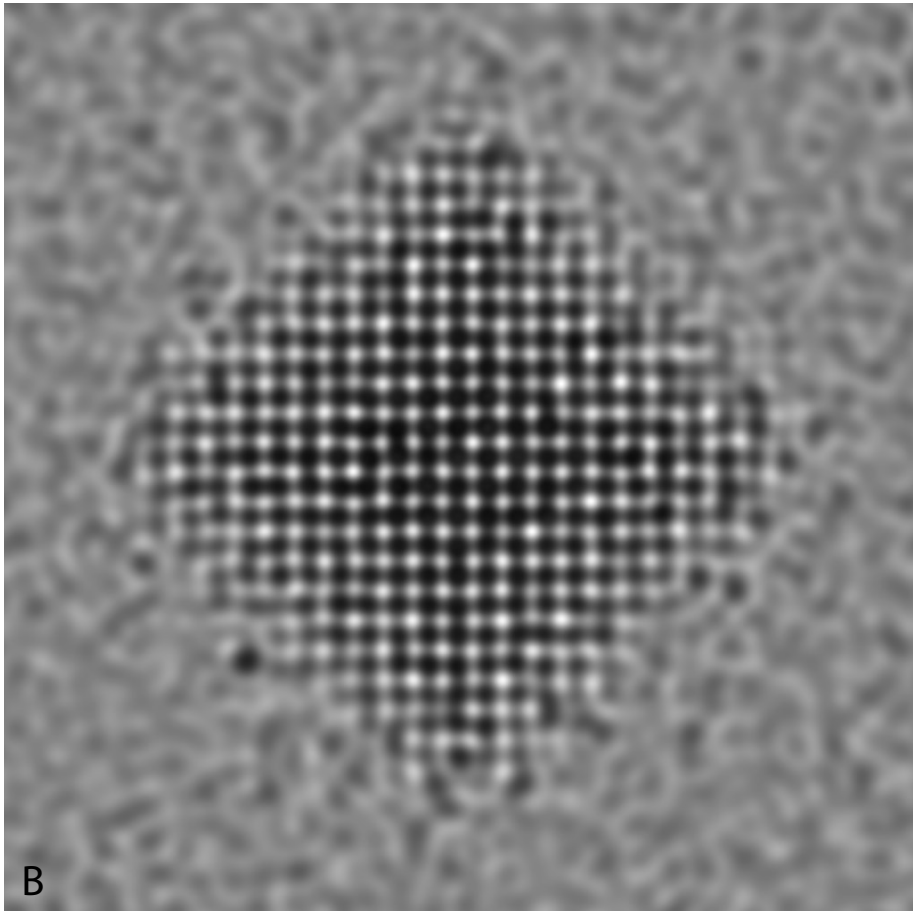

B

A: catalyst model (9500 atoms)

B: HREM image (Jeol 400kV).

This simulation was performed with a phase-object function sampled on a 1024 x 1024 grid.

Bloch wave method: z-independent potential

When the scattering potential is periodic, the eigenstates $|j>$ of the propagating electrons are Bloch waves. The hamiltonian of the system is projected on the eigenstates $|j>$ with eigenvalues γ_j (*"anpassung"* parameter).

$$\widehat{H} = \sum_j \gamma_j |j><j|$$

The evolution operator is then given by (since $V = V(\vec{\rho})$):

$$\widehat{U}(z,0) = e^{-i\widehat{H}z} = \sum_j e^{-i\gamma_j z}|j><j|$$

The wave-function at z developed on plane waves basis $|q>$:

$$\Psi(z) = \sum_q \phi_q(z)|q>$$

$$\phi_q(z) = < q|\widehat{U}(z,0)|0> = \sum_j e^{-i\gamma_j z} < q|j><j|0>$$

$$c_0^{*j} = < j|0> \text{ and } c_q^j = < q|j>$$

where in usual notation c_0^{*j} and c_q^j are the Bloch-wave excitations (component of the initial state $|0>$ on $|j>$) and coefficients (component of reflection $|q>$ on $|j>$) respectively[17].

[17] C. Humphreys & R.M. Fisher, Bloch Wave Notation in Many-Beam Electron Diffration, Acta Cryst. **A27** (1971) 42-45.

Bloch wave method: applications

Simulation of:

- SAED (kinematical and dynamical).
- CBED (polarity).
- LACBED (specimen thickness, symmetry).
- PED (Precession Electron Diffraction).
- HRTEM.

Works best for small lattice parameters crystals[18].

[18] Some more details in Appendix1.

CBED: ZnTe [110]

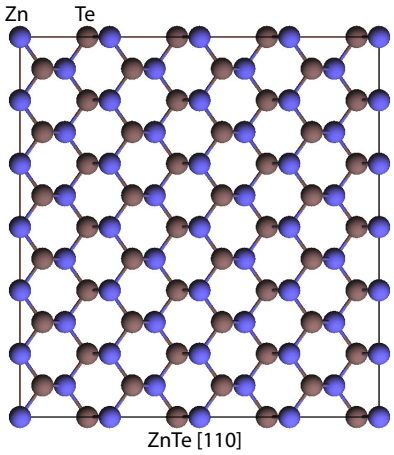

Figure: ZnTe [110].

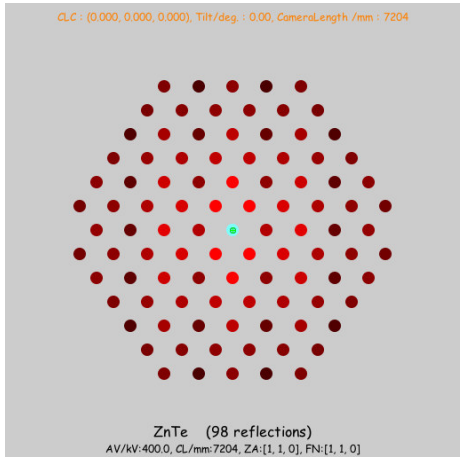

Figure: Reflections ($1 + 49$), $|\chi >= 0$.

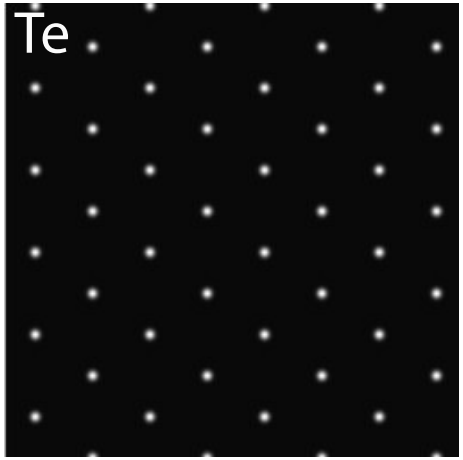

Figure: Bloch-wave 1 (Te 1s).

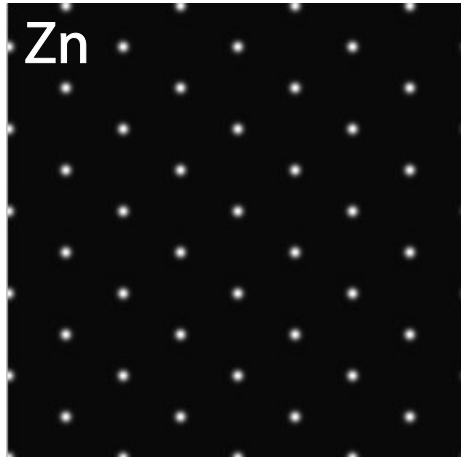

Figure: Bloch-wave 2 (Zn 1s).

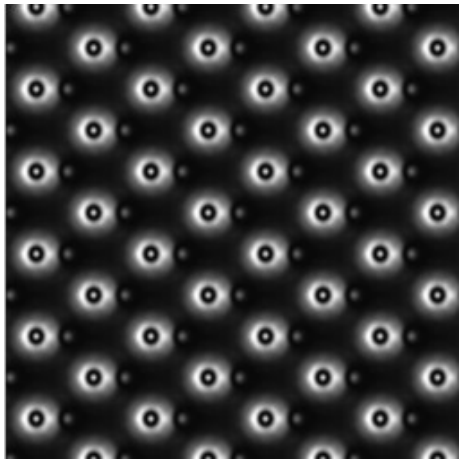

Figure: Bloch-wave 5 (Te-Zn).

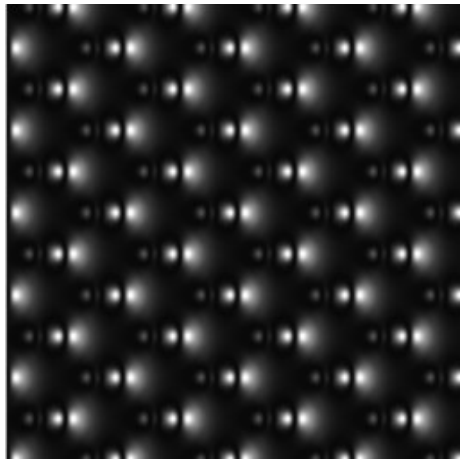

Figure: Bloch-wave 7 (Te-Zn).

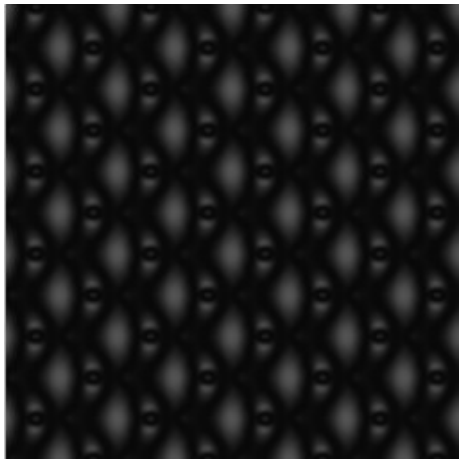

Figure: Bloch-wave 8 (Te-Zn).

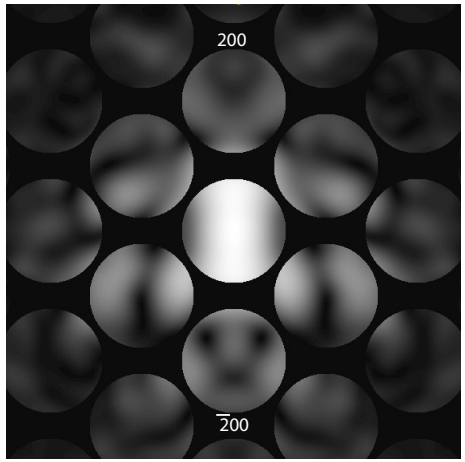

Figure: CBED (ZnTe polarity).

SAED: Diffraction pattern & specimen thickness

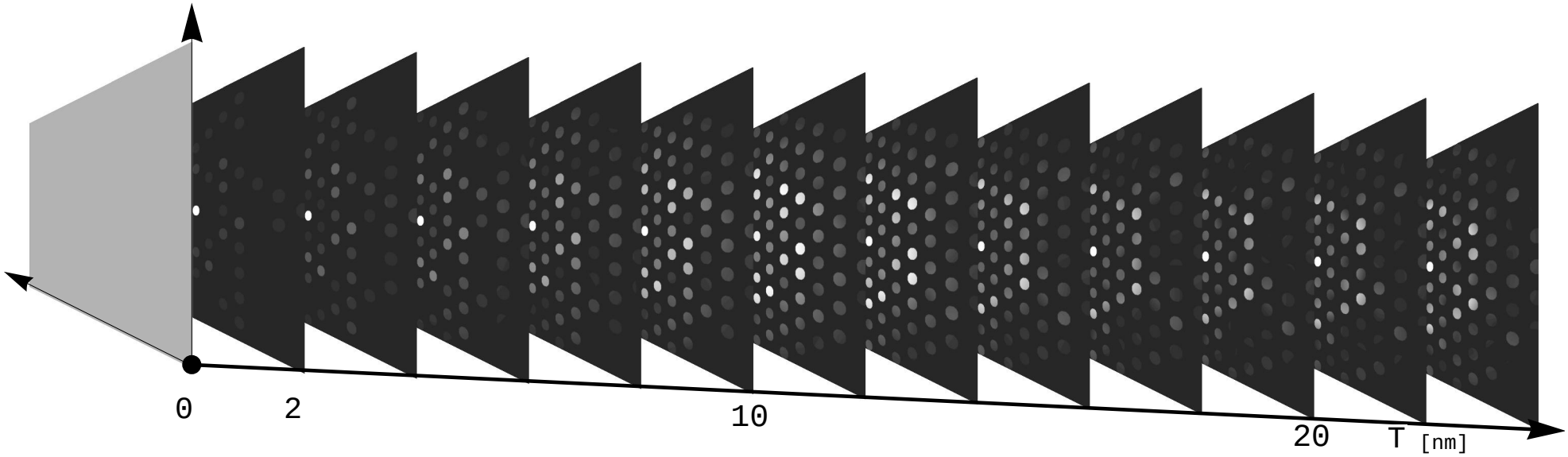

In BFP diffraction pattern depends specimen thickness.

Goodness of dynamical diffraction theories?

LACBED: Si [001]

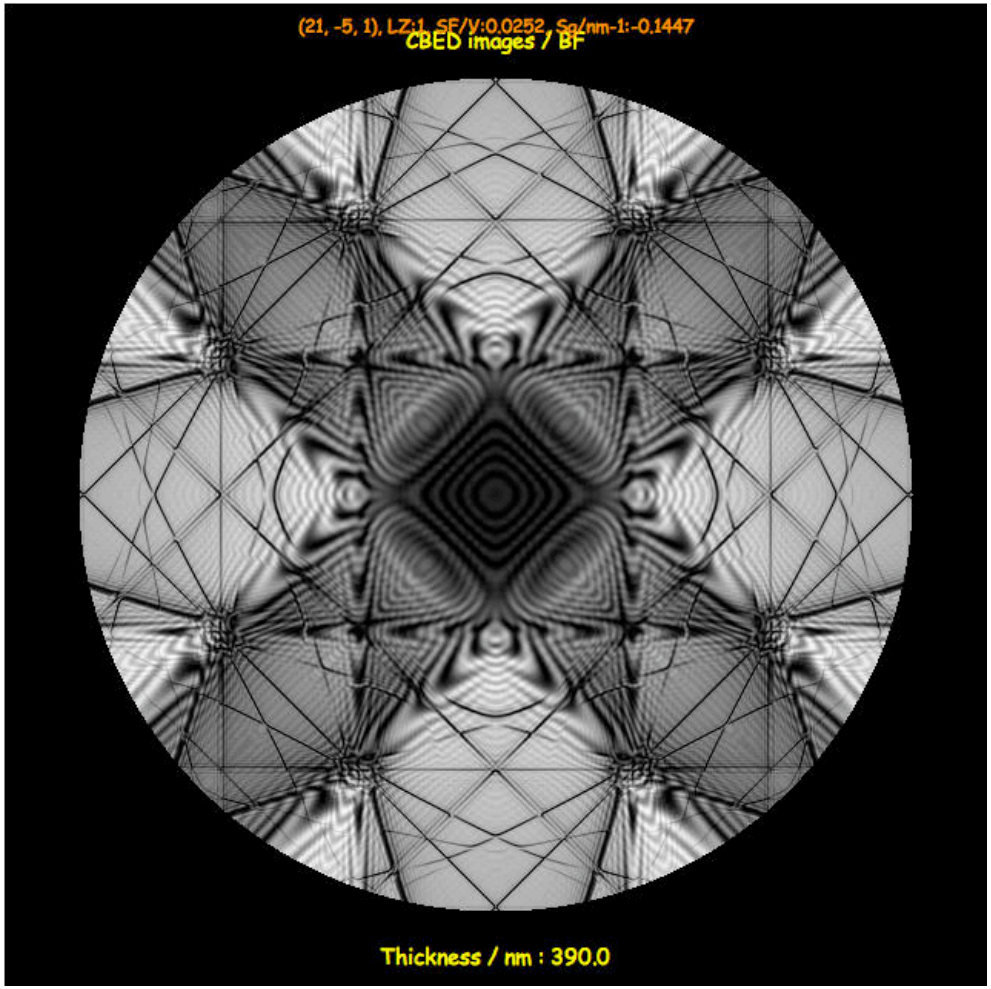

Figure: LACBED Si [001]: simulation.

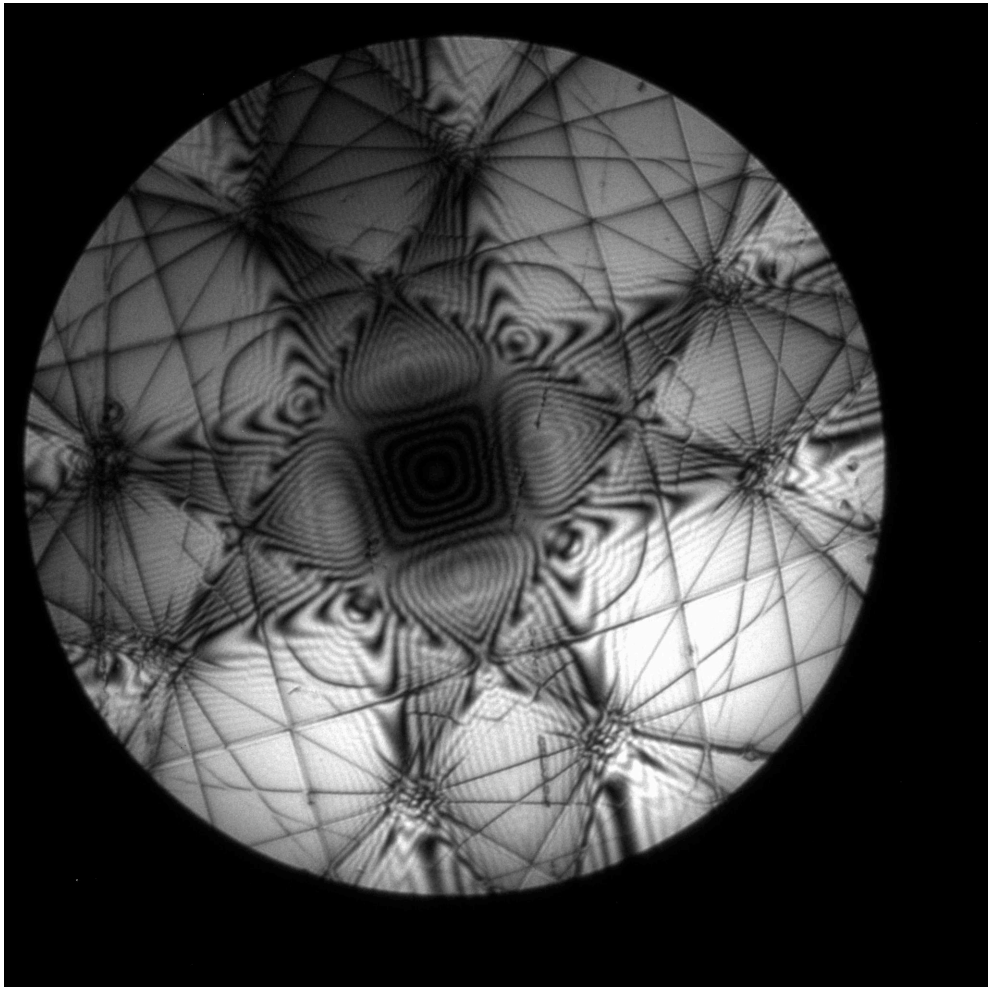

Figure: LACBED Si [001]: experimental (Web site EM centre - Monash university, J. Etheridge).

Note that the experimental LACBED pattern is blurred (inelastic scattering and/or MTF of CCD camera?).

Appendix 1: Dynamical theory of elastic scattering of high energy electron

We aim to understand in details multiple elastic scattering of electrons by crystals.

- High energy electron (eE).
- Periodic interaction potential $V(\vec{r})$.
- Time independent flux of incident electrons.

The fundamental equation of electron elastic scattering by a potential $V_v\,[Volt]$(positive inside a crystal) in the approximation of a stationary flux of electrons of a given energy $e\,E$ is the Schrödinger equation[19]:

$$\triangle\Phi(\vec{r}) + \frac{2me}{\hbar^2}[E + V_v(\vec{r})]\Phi(\vec{r}) = 0$$

With a change of notation its is written as:

$$[\triangle + 4\pi^2 K_i^2]\ \Phi(\vec{r}) = -4\pi^2 V_v(\vec{r})\ \Phi(\vec{r})$$

Where the wavevector $|\vec{K}_i|$ of the incident electrons is given by:

$$|K_i| = \frac{\sqrt{2meE}}{h}$$

and

$$m = \gamma\ m_0$$

[19] C. Humphreys, The scattering of fast electrons by crystals, Rep. Prog. Phys. **42** (1979) 1825-1887.

Schrödinger equation

The Laplacian $\triangle = \frac{\partial^2}{\partial x^2} + \frac{\partial^2}{\partial y^2} + \frac{\partial^2}{\partial z^2}$ is written as: $\triangle_\rho + \frac{\partial^2}{\partial z^2}$. As a result, $[\triangle + ...]e^{2\pi\imath k_z z}\Psi(\rho; z)$ is given by: $[\triangle_\rho + \frac{\partial^2}{\partial z^2} + ...]e^{2\pi\imath k_z z}\Psi(\rho; z)$.
Performing the z-differentiation:

$$\frac{\partial^2}{\partial z^2}e^{2\pi\imath k_z z}\Psi(\rho; z) = e^{2\pi\imath k_z z}[-4\pi^2 k_z^2 + 4\pi\imath k_z\frac{\partial}{\partial z} + \frac{\partial^2}{\partial z^2}]\Psi(\rho; z)$$

Inserting the last expression and dropping the term $e^{2\pi\imath k_z z}$:

$$[\triangle_\rho + 4\pi^2(K_i^2 - k_z^2 + V(\rho; z)) + 4\pi\imath k_z\frac{\partial}{\partial z} + \frac{\partial^2}{\partial z^2}]\Psi(\rho; z) = 0$$

Since $K_i^2 = k_z^2 + \chi^2$:

$$[\triangle_\rho + 4\pi^2\chi^2 + 4\pi^2 V(\rho; z) + 4\pi\imath k_z\frac{\partial}{\partial z} + \frac{\partial^2}{\partial z^2}]\Psi(\rho; z) = 0$$

Rearranging the last equation:

$$\imath\frac{\partial\Psi(\rho; z)}{\partial z} = -\frac{1}{4\pi k_z}[\triangle_\rho + 4\pi^2\chi^2 + 4\pi^2 V(\rho; z) + \frac{\partial^2}{\partial z^2}]\Psi(\rho; z)$$

Fundamental equation

$$\imath\frac{\partial\Psi(\rho;z)}{\partial z} = -\frac{1}{4\pi k_z}[\triangle_\rho + 4\pi^2\chi^2 + 4\pi^2 V(\rho;z) + \frac{\partial^2}{\partial z^2}]\Psi(\rho;z)$$

The term $|\frac{\partial^2\Psi(\rho;z)}{\partial z^2}|$ being much smaller than $|k_z\frac{\partial\Psi(\rho;z)}{\partial z}|$ we drop it (this is equivalent to neglect backscattering).

Fundamental equation of elastic scattering of high energy mono-kinetic electrons with a potential within the approximation of small angle scattering:

$$\imath\frac{\partial}{\partial z}\Psi(\rho;z) = -\frac{1}{4\pi k_z}[\triangle_\rho + 4\pi^2\chi^2 + 4\pi^2 V(\rho;z)]\Psi(\rho;z)$$

Time dependent Schrödinger equation $\Longrightarrow$ solution by many methods of quantum mechanics!

Remarks

- The approximations of the fundamental equation are equivalent to assume that the scattering potential is small compared to the accelerating potential and that k_z varies only slightly with z. It is in fact a quite good approximation, since the mean crystal potential is of the order of $10 - 20\ V$.
- Electron backscattering is neglected, the electron are moving forwards.
- The fundamental equation is actually equivalent to a 2-dimensional Schrödinger equation ($\rho = \{x, y\}$) where z plays the role of time. The system evolution is causal, from the past to the future.

Fundamental equation in Hamiltonian form:

$$\imath \frac{\partial}{\partial z} \Psi = H\ \psi$$

where:

$$H = -\frac{1}{4\pi k_z}[\triangle_\rho + 4\pi^2\chi^2 + 4\pi^2 V(\rho; z)] = H_o + \frac{4\pi^2 V(\rho; z)}{4\pi k_z}$$

A fundamental postulate of quantum mechanics[20] says that the evolution operator obeys the equation:

$$\imath \frac{\partial}{\partial z} U(z, 0) = H(\rho; z)\ U(z, 0)$$

[20] R. Shankar, Principles of Quantum Mechanics (1994) Plenum Press, New York and London.

Causal evolution operator

$U(z,0)$: unitary operator (the norm of $|\Psi>$ is conserved), in general not directly integrable $\Longrightarrow$ approximations.

$U(z,0)$ can be directly integrated only when $H(\rho;z)$ and $\frac{\partial}{\partial z}H(\rho;z)$ commute. In that case the general solution is[21]:

$$U(z,0) = e^{-\imath \int_0^z H(\tau)\, d\tau}$$

$H(\rho;z)$ and $\frac{\partial}{\partial z}H(\rho;z)$ commute when:

- $V(\rho;z)$ does not depend on z, i.e. $V(\rho;z) = V(\rho)$(perfect crystal).
- $V(\rho;z)$ can be neglected (free space propagation).
- $H(\rho;z)$ is approximated by it potential term (phase object).

Three approximations are available in jems:

- Multislice method.
- Bloch wave method.
- Howie-Whelan column approximation.

[21] A.Messiah, Mecanique quantique (1964) Dunod Paris.

jems student edition

To learn how to perform diffraction and image calculations (HRTEM and HRSTEM) you can download jems student edition version 4.4131 at:

http://www.jems-saas.ch/

Since we will use this software during the Hands-on demos, if you travel with your notebook either Windows, MacOSX or Linux ubuntu, have it installed on it.